# A century of mercury: Ecosystem-wide changes drive increasing contamination of a tropical seabird species in the South Atlantic Ocean

Fanny Cusset, S. James Reynolds, Alice Carravieri, David Amouroux, Océane Asensio, Roger Dickey, Jérôme Fort, B. John Hughes, Vitor Paiva, Jaime Ramos, et al.

# A century of mercury: Ecosystem-wide changes drive increasing contamination of a tropical seabird species in the South Atlantic Ocean

Fanny Cusset[1,2]*, S. James Reynolds[3,4], Alice Carravieri[1,2], David Amouroux[5], Océane Asensio[5], Roger C. Dickey[4], Jérôme Fort[1], B. John Hughes[3,4], Vitor H. Paiva[6], Jaime A. Ramos[6], Laura Shearer[7], Emmanuel Tessier[5], Colin P. Wearn[8], Yves Cherel[2] and Paco Bustamante[1,9]

[1] Littoral Environnement et Sociétés (LIENSs), UMR 7266 CNRS - La Rochelle Université, 2 rue Olympe de Gouges, 17000 La Rochelle, France

[2] Centre d'Études Biologiques de Chizé (CEBC), UMR 7372 CNRS - La Rochelle Université, 79360 Villiers-en Bois, France

[3] Centre for Ornithology, School of Biosciences, College of Life & Environmental Sciences, University of Birmingham, Edgbaston, Birmingham, UK

[4] Army Ornithological Society (AOS), c/o Prince Consort Library, Aldershot, Hampshire, UK

[5] Institut des Sciences Analytiques et de Physico-Chimie pour l'Environnement et les Matériaux (IPREM), UMR 5254, CNRS, Université de Pau et des Pays de l'Adour, Pau, France

[6] University of Coimbra, MARE – Marine and Environmental Sciences Centre / ARNET - Aquatic Research Network, Department of Life Sciences, Calçada Martim de Freitas, 3000-456 Coimbra, Portugal

[7] Ascension Island Government Conservation and Fisheries Directorate (AIGCFD), Georgetown, Ascension Island, South Atlantic Ocean

[8] The Royal Air Force Ornithological Society (RAFOS), High Wycombe, Buckinghamshire, UK

[9] Institut Universitaire de France (IUF), 1 rue Descartes 75005 Paris, France

*Corresponding author: fanny.cusset1@univ-lr.fr

**ABSTRACT:** Mercury (Hg) is a highly toxic metal that adversely impacts human and wildlife health. The amount of Hg released globally in the environment has increased steadily since the Industrial Revolution, resulting in growing contamination in biota. Seabirds have been extensively studied to monitor Hg contamination in the world's oceans. Multidecadal increases in seabird Hg contamination have been documented in polar, temperate and subtropical regions, whereas in tropical regions they are largely unknown. Since seabirds accumulate Hg mainly from their diet, their trophic ecology is fundamental in understanding their Hg exposure over time. Here, we used the sooty tern (*Onychoprion fuscatus*), the most abundant tropical seabird, as bioindicator of temporal variations in Hg transfer to marine predators in tropical ecosystems in response to trophic changes and other potential drivers. Body feathers were sampled from 220 sooty terns, from museum specimens (n=134) and free-living birds (n=86) from Ascension Island, in the South Atlantic Ocean, over 145 years (1876-2021). Chemical analyses included (i) Hg (total- and methyl-Hg), and (ii) carbon ($\delta^{13}C$) and nitrogen ($\delta^{15}N$) stable isotopes, as proxies of foraging habitat and trophic position, respectively, to investigate the relationship between trophic ecology and Hg contamination over time. Despite current regulations on its global emissions, mean Hg concentrations were 58.9% higher in the 2020s (2.0 µg/g, n=34) than in the 1920s (1.2 µg/g, n=107). Feather Hg concentrations were negatively and positively associated with $\delta^{13}C$ and $\delta^{15}N$ values. The sharp decline of 2.9 ‰ in $\delta^{13}C$ values over time indicates ecosystem-wide changes (shifting primary productivity) in the tropical South Atlantic Ocean and can help explain the observed increase in tern's feather Hg concentrations. Overall, this study provides invaluable information on how ecosystem-wide changes can increase Hg contamination of tropical marine predators and reinforces the need for long-term regulations of harmful contaminants at the global scale.

**KEYWORDS:** Feathers – Hg – Museum– Sooty tern – Stable isotopes – Temporal monitoring

## INTRODUCTION

Mercury (Hg) is a toxic metal and its impacts on human health are a major concern. Globally, the amount of Hg released into the environment has steadily increased since the Industrial Revolution, resulting in a three- to five-fold increase of Hg on land, in the atmosphere and the ocean (Lamborg et al., 2014; Selin, 2009). Since Hg is primarily emitted in the atmosphere in its volatile form ($Hg^0$) by both natural and human sources (Eagles-Smith et al., 2018) where it remains for up to one year (Streets et al., 2019), it disperses widely before its deposition in all global ecosystems. Consequently, even remote oceanic regions are affected by this global pollutant. Once in the sea, Hg is methylated by microorganisms into methyl-Hg (MeHg), its most toxic and bioavailable form. Because of its high assimilation efficiency and strong affinity for proteins, MeHg bioaccumulates in marine organisms (*i.e*., concentrations increase over time in their tissues) and biomagnifies in food webs (*i.e.,* concentrations increase at each elevated trophic level). Marine food resources represent the principal source of Hg for humans and wildlife. Mercury can cause severe physical and neurological harm and even mortality at sufficiently high concentrations, as is the case in Minamata Disease (Takeuchi et al., 1962). This has led to new regulations, such as the Minamata Convention on Mercury, to protect human health and the environment, by controlling and reducing anthropogenic releases of Hg globally.

Oceans receive 80% of total atmospheric Hg deposition, 49% of which is restricted to tropical oceans (Horowitz et al., 2017). Despite this, little is known about the interactions between Hg and ecosystem function in the intertropical zone. Yet, it is here that artisanal and small-scale gold mining occurs, resulting in annual Hg emissions >720 tonnes. Gold mining is the largest contributor to Hg emissions and represents >35% of total global anthropogenic Hg

emissions (Eagles-Smith et al., 2018). In addition, tropical oceans have recently experienced increased oxygen-depletion (Breitburg et al., 2018), creating favourable conditions for MeHg formation (Cossa, 2013; Mason et al., 2012; Sunderland et al., 2009). Quantifying Hg contamination and its temporal trends in tropical oceans and wildlife is thus urgently needed.

Monitoring tropical oceans is logistically challenging but can be achieved through investigations of bioindicators that feed extensively across their waters and, thus, provide a lens through which to investigate Hg contamination. Seabirds are effective bioindicators (Burger and Gochfeld, 2004; Furness, 1993) because of their high position in marine trophic webs and longevity, allowing them to integrate and reflect Hg contaminations of their food webs (Fort et al., 2016; Furness and Camphuysen, 1997; Piatt et al., 2007). Furthermore, most seabirds are colonial (*i.e.*, they concentrate in high numbers in breeding colonies) and philopatric (*i.e.*, they have high site fidelity). Thus, several individuals can be sampled simultaneously, and repeatedly through time, in particular through non-lethal collection of feathers (Albert et al., 2019). Feathers are a reliable tissue to investigate Hg contamination in seabirds (Thompson et al., 1998), because dietary MeHg accumulates in body tissues between moulting episodes (Furness et al., 1986). Up to 90% of the accumulated MeHg is sequestered into growing feathers after transportation in the blood and then excreted during moult (Honda et al., 1986). In feathers, MeHg binds to sulfhydryl groups of keratin molecules (Crewther et al., 1965) to form strong, stable bonds that withstand rigorous physical treatments over time (Appelquist et al., 1984). Mercury contained in feathers is mostly in the form of MeHg (>90%, Renedo et al., 2017) and thus seabird feathers are commonly used for Hg biomonitoring over the short- and the long-term (*e.g.*, Albert et al., 2019; Burger and Gochfeld, 2004; Cherel et al., 2018).

Seabirds have been collected for exhibitions and museum collections worldwide over the last centuries and, therefore, their specimens are invaluable to study temporal trends of Hg contamination (Vo et al., 2011). However, inorganic Hg salts were used historically by museum curators as preservatives in specimen preparation, resulting in methodological bias when analysing museum *versus* free-living specimens. This bias can be overcome by analysing MeHg specifically (Hogstad et al., 2003). Overall, only a limited number of studies (n=14) have quantified Hg in museum-held seabird specimens over the last century, and only four of these have considered trophic ecology as a factor that could influence Hg contamination (see Supplementary Material, Table S1 for species and temporal comparisons). Yet, bird trophic ecology is key to understanding the mechanisms of Hg contamination and to disentangle whether temporal variations in Hg contamination are linked to dietary shifts and/or to changes in environmental Hg contamination (Bond et al., 2015; Carravieri et al., 2016; Choy et al., 2022; Fort et al., 2016; Vo et al., 2011). Over multidecadal timescales, decreases and stable trends in Hg contamination have been documented in only one temperate Atlantic species (Thompson et al., 1992) and one temperate Pacific species (Choy et al., 2022), respectively. In contrast, increases in Hg contamination have been observed in 12 temperate Atlantic species ( Monteiro and Furness, 1997; Thompson et al., 1992; Thompson et al., 1993), one temperate/subtropical Pacific species (Vo et al., 2011) and one Arctic species (Bond et al., 2015). Notably, none of these studies involved long-term investigation of tropical regions.

The sooty tern (*Onychoprion fuscatus*) is the most abundant tropical seabird, widely distributed in all three ocean basins. This species is therefore an ideal candidate to monitor Hg contamination in tropical food webs. The present work extends the investigation of Reynolds et al. (2019), who highlighted long-term changes in the feeding ecology of sooty terns breeding on

Ascension Island (the largest colony in the South Atlantic Ocean), by using carbon ($\delta^{13}C$) and nitrogen ($\delta^{15}N$) stable isotopes, which are proxies of feeding habitat (*i.e.,* carbon source) and diet (*i.e.,* trophic position), respectively (Kelly, 2000). Reynolds et al. (2019) found long-term declines in both feather $\delta^{13}C$ and $\delta^{15}N$ values since the 1890s, indicating a fundamental change in their foraging behaviour, including a dietary shift from predominantly teleost fish to squid coinciding with a dramatic decline in the size of the breeding population on Ascension Island. Here, our aim was three-fold to: (i) document the temporal trend of feather Hg concentrations in Ascension sooty terns between the 1890s and the 2020s, (ii) investigate the influence of their trophic ecology (reflected by $\delta^{13}C$ and $\delta^{15}N$ values) on this temporal trend and (iii) compare feather Hg contamination before and after population collapse. As for other remote oceanic regions, we predict that there will be a general increase in feather Hg concentrations to the present day, linked to the previously documented changes in their diet and foraging behaviours.

## MATERIALS AND METHODS

### Study area and museum specimens

Ascension Island (07°57′ S, 14°24′ W) is an isolated 97 $km^2$ volcanic island in the tropical South Atlantic Ocean. It accommodates the largest breeding population of sooty terns in the entire Atlantic Ocean, containing on average >200,000 pairs (Hughes et al., 2012). Currently, they nest on bare ground across the Wideawake Fairs – an Important Bird Area (IBA SH009) – at two Nature Reserves (NRs) called Mars Bay and Waterside Fairs. As epipelagic seabirds, sooty terns feed on small pelagic fish and squid caught at or near the ocean surface (Ashmole, 1963a; Reynolds et al., 2019). Globally, sooty terns are listed as of 'Least Concern' in the IUCN Red List of Threatened Species. Yet, the population from Ascension Island has drastically declined by approximately 84% between the 1960s and 1990s from a peak of approximately two million birds

(Hughes et al., 2017). Many factors may have contributed to this precipitous decline, including the depletion of food resources and predation by introduced species such as domestic cats (*Felis silvestris catus*), black rats (*Rattus rattus*) and common mynas (*Acridotheres tristis*) (Reynolds et al., 2019 and references therein).

**Feather sampling and preparation**

Sooty terns from Ascension Island breed sub-annually (~10 months; Reynolds et al., 2014). While still breeding, they start their post-nuptial moult (*i.e.,* basic moult) and replace all of their feathers (flight and body feathers) during the following weeks/months (Ashmole, 1963b). Therefore, body feathers collected during the breeding season provide information on bird Hg exposure since the previous moult (*i.e*. for the past 10 months; Albert et al., 2019). This includes different stages of their life cycle: (i) the end of the previous breeding season, (ii) the post-breeding migration, (iii) the non-breeding period, (iv) the pre-breeding migration and (v) the beginning of the current breeding season. Consequently, feathers also provide information at different spatial scales, since sooty terns have a maximum non-breeding range of 2,900 km in tropical waters around Ascension Island (Reynolds et al., 2021). Feathers also retain dietary signatures at the time of their synthesis, as carbon and nitrogen isotopes are incorporated into feathers as they grow *(i.e*., over a few weeks). Consequently, Hg concentrations and stable isotope values of feathers are temporally decoupled (Thompson et al., 1998, Bond 2010). Nonetheless, stable isotope values can provide invaluable information about seabird foraging ecology across century scales by virtue of their constant integration over time, therefore allowing for long-term understanding of Hg temporal trends.

Historical feather samples were collected from skins held in 10 natural history museum collections (see details in Supplementary Table S2). Details of museum skins are provided in

Supplementary Table S3. The complete procedure for historical sampling and preparation is detailed in Reynolds et al. (2019). Only specimens with known collection date (*i.e.*, year or decade) were considered for the current study. When the precise year of specimen collection was unknown (n=7), we attributed the first year of the corresponding decade to it. Sex of birds from which skins were prepared was known for some historical samples (*i.e.*, 43 females and 41 males from the 1920s). Feather sampling of free-living birds was carried out at Mars Bay NR and Waterside Fairs NR breeding colonies in 2006 by BJH (n=8), 2012 by CPW and SJR (n=40) and 2020 (n=4) and 2021 (n=30) by LS. These samples were collected by licenced professionals under environmental research permits issued by Ascension Island Government. Incubating sooty terns were caught during ringing activities using a soft mesh hand-held net. While processing the birds (Redfern and Clark, 2001), contour feathers were removed from across the breast on both sides of the keel ridge. Samples were collected from breeding adults and stored at room temperature prior to preparation and analysis.

To eliminate any external contamination, all feathers were cleaned in the laboratory with a chloroform:methanol mixture (2:1), sonicated for 3 min and rinsed twice in methanol. They were then oven-dried for 48h at 45°C. For each bird specimen, several feathers (2-4) were pooled to derive the individual mean value (Carravieri et al., 2014; Jaeger et al., 2009), then cut with stainless scissors into a homogeneous powder to be analysed for both stable isotopes and Hg.

**Stable isotope analyses**

Carbon and nitrogen stable isotopes were analysed in homogenized subsamples of body feathers. Results are expressed in the δ unit notation as deviations from standards (Vienna Pee Dee Belemnite for $\delta^{13}C$ and atmospheric $N_2$ for $\delta^{15}N$) following the formula:

$$\delta^{13}C \text{ or } \delta^{15}N = (R_{sample}/R_{standard} - 1) \times 10^3$$

where R is $^{13}C/^{12}C$ or $^{15}N/^{14}N$, respectively. Analyses of historical samples (*i.e.*, from the 1890s to the 2010s) were performed at the MARE and results were presented in Reynolds et al. (2019). The present study extends this previous investigation by another decade to the present day. Analyses of these contemporary feathers (*i.e.,* from the 2020s) were performed at the LIENSs. Feather subsamples (~0.4 mg) were weighed with a microbalance and loaded into tin cups. Values of $\delta^{13}C$ and $\delta^{15}N$ were determined with a continuous flow mass spectrometer (Delta V Plus with a Conflo IV Interface, Thermo Scientific, Bremen, Germany) coupled to an elemental analyzer (Flash 2000 or EA Isolink, Thermo Scientific, Milan, Italy). The analytical precision was <0.10 ‰ and <0.15 ‰ for $\delta^{13}C$ and $\delta^{15}N$ values, respectively. Ten samples were analysed in both laboratories to compare analytical performances. No difference in $\delta^{13}C$ (ANOVA, $F_{1,18}$=0.04, p=0.80) nor $\delta^{15}N$ values (ANOVA, $F_{1,18}$=0.008, p=0.90) was detected between the two laboratories, ensuring data comparability between the older (from Reynolds et al., 2019) and most recent feather samples.

Since the Industrial Revolution, the combustion of human fossil fuel has increased atmospheric $CO_2$, resulting in an accelerating decrease in biosphere $\delta^{13}C$, mainly influenced by two additive effects: (i) an increase in phytoplankton fractionation (Rau et al., 1992), and (ii) the so-called «Suess-Effect» (Keeling, 1979), whereby anthropogenic carbon has lower $\delta^{13}C$ values than natural background carbon. In our study, raw $\delta^{13}C$ values were thus corrected accordingly, following calculations from previous work (Eide et al., 2017; Hilton et al., 2006; Jaeger and Cherel, 2011; Körtzinger et al., 2003). For further information, please see Supplementary Figure S1 for a comparison of isotopic niches of raw and corrected $\delta^{13}C$ values.

**Mercury analyses**

Generally, total Hg (THg) includes both inorganic (iHg) and organic Hg (*i.e.,* MeHg). In feathers, MeHg accounts for >90% of THg (Bond and Diamond, 2009; Renedo et al., 2017; Thompson and Furness, 1989). So, THg can be used as a proxy of MeHg in feathers. Here, THg analyses were performed on homogenized feathers using an Advanced Mercury Analyser spectrophotometer (Altec AMA 254). Each sample was analysed in duplicate-triplicate to guarantee a relative standard deviation <10%. Accuracy was verified by running certified reference material (DOLT-5, Fish liver, National Research Council, Canada: certified Hg concentration = 0.44 ± 0.18 µg $g^{-1}$ dry weight [dw]). Our measured values were 0.43 ± 0.01 µg $g^{-1}$ dw (n=14). Blanks were run at the beginning of each set of samples. Detection limit of the AMA was 0.01 ng. Mercury concentrations are expressed in µg $g^{-1}$ dw.

Historically, inorganic Hg salts were used as preservatives in museum collections until approximately the 1970s, creating a major bias in THg comparison between old and recent specimens (Thompson et al., 1992). Therefore, Hg speciation analyses were performed on the oldest specimens (n=131; until the 1970s) to quantify both MeHg and iHg (Renedo et al. 2017, 2018) from feather homogenates (1.1−12.0 mg), using an GC-ICP-MS Trace Ultra GC equipped with a Triplus RSH autosampler coupled to an ICP-MS XSeries II (Thermo Scientific, USA). Mercury speciation analyses were also performed on a few free-living individuals (n=3, from the 2000s) to determine the precise proportion of MeHg in sooty tern feathers and hence validate the use of THg as proxy of MeHg after the 1970s. Further methodological details are provided in Supplementary Material, including a comparison of speciation results between old and recent specimens (Table S4). Certified reference material (NIES-13, human hair; certified MeHg concentration = 3.80 ± 0.40 µg $g^{-1}$ dw) was analysed for validation of feather analyses (keratin-

based matrices). Our measured concentrations for MeHg were 3.64 ± 0.09 µg $g^{-1}$ dw (n=3). Method recovery was checked by comparison of THg values measured with AMA and the equivalent Σ MeHg + iHg obtained from speciation analyses. Further details on recovery calculations are shown in Table S5. Average recovery of sooty tern feather Hg was 96.1 ± 4.9% (92.3−101.3%; n=3; see Supplementary Material). Thereafter, feather Hg concentrations include MeHg and THg concentrations from birds collected until and after the 1970s, respectively.

**Data analyses**

All statistical analyses and graphical representations were carried out in R 4.0.3 (R Core Team, 2020).

Temporal trends of Hg and stable isotopes over 145 years

Year-specific sample sizes were unbalanced (Table 1), with five times more observations on average in 1925 than in other years. Thus, 50 values were randomly extracted from this specific year and used in all models. One outlier was identified in 1915 (*i.e.,* JR11, Table S3) and removed from all analyses. Data exploration revealed that Hg, $\delta^{13}C$ and $\delta^{15}N$ varied non-linearly with time. Therefore, Generalized Additive Models (GAMs) were run to investigate non-linear temporal trends over 145 years, using the « mgcv » package (Wood, 2011). Each variable was modeled independently against year as a smoother. For each model, we adapted the smoothed term (k) to avoid overfitting and oversimplification, and obtain the best and most realistic fit to the data (k=5 for Hg, $\delta^{13}C$ and $\delta^{15}N$ values). Model assumptions were checked *via* residual analysis through the « gam.check » function.

Drivers of Hg contamination over time

Multifactorial analyses were used to test for the effect of trophic ecology on feather Hg concentrations over time. To discard the combined effect of time on both feeding habitat and trophic position, we detrended all variables by extracting residuals from GAM temporal trends of Hg, $\delta^{13}C$ and $\delta^{15}N$ values. The new response variable was time-detrended Hg concentrations and continuous explanatory variables were the time-detrended $\delta^{13}C$ and $\delta^{15}N$ values. Relationships between detrended variables were then investigated with linear models using the « nlme » package (Pinheiro et al., 2020). Prior to model construction, one-way ANOVA was used to test for differences in Hg concentrations between the sexes of terns. As no difference was detected ($F_{1,82}$=2.82, p=0.10; Supplementary Figure S2), sex was not included in model selection procedures. Models were GAMs with a Gaussian distribution and an identity link function. The initial model was: detrended Hg ~ detrended $\delta^{13}C$ + detrended $\delta^{15}N$. All potential combinations of variables (Table 2) were subjected to model selection based on the Akaike's Information Criterion adjusted for small sample sizes ($AIC_c$), using the « MuMIn » package (Bartón, 2022). The model with the lowest $AIC_c$ value, with a difference of $AIC_c$ of two or more compared to the next model (ΔAICc), was selected as the best model (Burnham and Anderson, 2002). Model performance was assessed using Akaike weights ($w_i$) (after Johnson and Omland, 2004) and model fit was checked by residual analysis of the initial model.

To compare temporal trends with the published literature, we calculated the percentage of change (increase or decrease) for evolution phases identified by GAM temporal trends. Details of empirical calculations are provided in the Supplementary Material (Table S6).

Temporal comparison: before and after population collapse

Following Reynolds et al. (2019), we tested for differences in trophic ecology and Hg concentrations of sooty terns relative to their population collapse on Ascension Island (*i.e.,* before: 1890s−1940s; after: 1970s−2020s). First, a Multivariate Analysis of Variance (MANOVA) enabled us to test for differences in isotopic niches (*i.e.,* $\delta^{13}C$ and $\delta^{15}N$ values combined) between periods. Differences between periods for individual isotopes were then identified using the « summary.aov » function. Residual normality (« mvnormtest package »; Jarek, 2012), outliers (« rstatix » package; Kassambara, 2021) and multicollinearity (between $\delta^{13}C$ and $\delta^{15}N$ values; « cor.test » function) were checked prior to interpretation. Secondly, one-way ANOVA was used to test for differences in Hg concentrations between the two periods. Prior to model construction, normality of residuals and homoscedasticity were tested with Shapiro and Breush-Pagan tests, respectively. An alpha threshold of 0.05 was used for all statistical analyses.

## RESULTS

Temporal trend of Hg contamination and trophic ecology

Body feathers were sampled from 220 sooty terns from seven different decades, spanning 145 years (*i.e.,* 1876-2021; Table 1), from museum skins (n=134) and free-living birds (n=86). Few data were available prior to the 1920s, leading to high variability and large uncertainty in temporal trends of Hg concentrations before the 1920s (Figure 1A). Thus, interpretation of GAM temporal trends could only be carried out from the 1920s onwards. For this reason, results

presented here mainly focus on the period between the 1920s and the 2020s. Detailed outputs from GAMs describing temporal variations in Hg, $\delta^{15}N$ and $\delta^{13}C$ values are provided in Table S7.

Since the 1920s, Hg concentrations increased non-linearly with time (GAM, $p<0.0001^{***}$, deviance explained was 0.25), following three distinct phases. First, Hg concentrations increased by 62.9% between the 1920s and the 1970s. Then, Hg concentrations exhibited an unclear pattern of change between the 1970s and the 2000s with high variability and large confidence intervals. Finally, Hg concentrations increased again by 62.8% from the 2000s to the present day. Overall, Hg concentrations were 58.9% higher in the 2020s than in the 1920s.

The $\delta^{15}N$ values ranged from 9.49 ‰ in the 2010s to 15.42 ‰ in the 1890s (Figure 1B), with values varying non-linearly over time (GAM, $p<0.0001^{***}$, deviance explained was 0.13), following three distinct phases. Values of $\delta^{15}N$ increased by 5.8% between 1920s and the 1940s (i.e., +0.75 ‰), decreased by 10.4% thereafter until the 2000s (i.e., −1.34 ‰) and increased by 11.5% from 2000s (i.e., +1.33 ‰) to the present day (Tables 1 and S6).

Corrected $\delta^{13}C$ isotopic values ranged between –17.4 ‰ in the 2010s and –11.9 ‰ in the 1920s (Figure 1C), with values decreasing dramatically over time (GAM, $p<0.0001^{***}$, deviance explained was 0.91). There was a quasi-linear 17.4% change over the century between the 1920s and the 2020s (i.e., +2.85 ‰).

Feather Hg concentrations were 38.8% higher after (1.79 ± 0.48 µg $g^{-1}$ dw) than before (1.29 ± 0.46 µg $g^{-1}$ dw) (ANOVA; $F_{1,218}=59.2$, $p<0.001^{***}$) the population collapse that occurred between the 1960s and the 1990s (Figure 2A). Isotopic niches were statistically different before and after the population collapse (MANOVA; $F_{1,218}=649.8$, $p<0.0001^{***}$; Figure 2B), with no

significant difference in $\delta^{15}N$ values (–0.7%; p=0.39) and ~2.5 ‰ lower $\delta^{13}C$ values after than before the population collapse (–18.6%; ANOVA; $F_{1,218}$=1271.8, p<0.001$^{***}$).

Drivers of Hg contamination over time

Results from model selection are provided in Table 2. The best model to explain time-detrended Hg concentrations included both time-detrended $\delta^{13}C$ and $\delta^{15}N$ values (linear models, $R^2$=0.14, p < 0.0001$^{***}$). Specifically, Hg concentrations decreased with increasing $\delta^{13}C$ values ($\beta$ ± SE, -0.279 ± 0.082, 95% CI: −0.442, −0.117) and increased with increasing $\delta^{15}N$ values ($\beta$ ± SE 0.090 ± 0.030, 95% CI: 0.031, 0.149) (Figure 3).

## DISCUSSION

In this study, sooty terns act as bioindicators of temporal trends in Hg contamination of food webs in the tropical South Atlantic Ocean. We have built on previous long-term investigations of the trophic ecology of breeding sooty terns on Ascension Island (1890s-2010s; Reynolds et al., 2019), by extending the recent time series by an additional decade and providing feather-derived Hg concentrations. To the best of our knowledge, this is the first study to determine Hg contamination over such an extensive multidecadal timescale in the tropical oceans. Our results revealed a global non-linear increase in Hg contamination of sooty terns over the last 145 years, because of both trophic and environmental changes over time.

Museum specimens represent invaluable archives that enable both dietary and ecotoxicological investigations on multidecadal timescales. However, any retrospective investigation at a single location is challenging, because it is highly dependent on sampling effort each year over a large time scale. Gaps in retrospective time-series are thus very common and

consequently, analytical statistical approaches such as non-linear approaches appeared as the most relevant. Because the oldest specimens in our study were also the least numerous, temporal trends were characterized by high uncertainty between the 1890s and the 1920s (Figure 1A). For this reason, interpretations of our findings mainly focussed on the 1920s to the 2020s.

**Long-term trend in foraging ecology: an update**

Using feathers as a record of sooty tern foraging ecology on the island, Reynolds et al. (2019) found a significant decrease in feather $\delta^{15}N$ values, suggesting a change in their trophic position over time. By extending the time series in this study with the inclusion of feathers obtained in 2020 and 2021, we did not detect any further significant linear trend in $\delta^{15}N$ values. Instead, we detected a non-linear trend (Figure 1B): initially, there was an increase between the 1900s and the 1940s, followed by a decrease between the 1940s and the 2000s, and a second increase from the 2000s onwards (Table 1 and S6). The addition of the most recent decade in the time series clearly highlights the importance of such long-term monitoring, by revealing recent and unpredictable patterns in the foraging ecology of sooty terns. These long-term variations in feather $\delta^{15}N$ values could reflect variations in seabird diet over time (Reynolds et al., 2019), but also changes in the isotopic baseline (McMahon et al., 2013). Isoscapes of $\delta^{15}N$ can vary seasonally due to changes in primary productivity which stem from variation and cycling of nutrient sources, as well as changes in species composition and growth rates of phytoplankton (Cifuentes et al., 1988; Goering et al., 1990; Ostrom et al., 1997; Vizzini and Mazzola, 2003). The changing $\delta^{15}N$ isoscape could then have cascading effects on feather isotopic values of seabird consumers at upper trophic levels and hence, drive the temporal variations in their trophic position. One way to disentangle these hypotheses would be to perform compound-specific stable isotope analysis of amino acids (CSIA-AA) (McMahon and Newsome, 2019), which would help

distinguish the specific signatures of the baseline («source» $\delta^{15}$N-AAs) and the diet-consumer transfer («trophic» $\delta^{15}$N-AAs), and hence elucidate the «true» trophic position of sooty terns over time.

Extending the results of Reynolds et al. (2019), corrected $\delta^{13}$C values exhibited a similar and even stronger decreasing trend to the present day (Figure 1C), with a 2.85 ‰ decline between the 1920s and the 2020s. This represents a 3.24 ‰ decline when considering the trend between the 1890s and the 2020s. A comparable decrease in $\delta^{13}$C values over time was previously described in thin-billed prions (*Pachyptila belcheri*) in the Southern Ocean (Cherel et al., 2014; Quillfeldt et al., 2010), and was interpreted as a result of latitudinal change in their moulting area, switching from sub-Antarctic to Antarctic waters over more than 90 years (1913-2005). Similarly, moulting areas of Ascension sooty terns could have changed spatially over time but, to date, their post-breeding migrations have only been studied using geolocators between 2011 and 2015 (Reynolds et al., 2021) and far more research is required. Continuing such tracking work over the next few decades would allow trophic ecology of sooty terns to be directly related to long-term changes in their spatial distribution in the South Atlantic Ocean. Alternatively and similar to the hypothesis generated above for changes in feather $\delta^{15}$N values, changes in $\delta^{13}$C values might reflect baseline changes in the study area. Baseline $\delta^{13}$C values vary both spatially (latitudinal gradient influenced by temperature; Sackett et al., 1965) and temporally (seasonal variability) in the marine environment (McMahon et al., 2013). The temporal decline in $\delta^{13}$C values of sooty terns could thus reflect fluctuations in baseline $\delta^{13}$C values. However, the observed trend appears too marked to be explained solely by a change in $\delta^{13}$C baseline values. Carbon isotope values reflect phytoplankton productivity in aquatic environments (DeNiro and Epstein, 1978; France, 1995; Hobson, 1999). Declines in $\delta^{13}$C values have been associated with

those in primary productivity, and hence with the carrying capacity of ecosystems (Hirons et al., 2001; O'Reilly et al., 2003; Schell, 2000), and ultimately with declines of penguin (Spheniscidae) populations, for example, in the sub-Antarctic region (Hilton et al., 2006; Jaeger and Cherel, 2011). In the South Atlantic Ocean, a 1.38 ‰ decline in $\delta^{13}C$ values was observed in muscle of tuna species in the between 2000 and 2015, suggesting a global shift in phytoplankton community structure (Lorrain et al., 2020). This coincides with the 1.24 ‰ decline we observed in feather $\delta^{13}C$ values of Ascension sooty terns between the 2000s and the 2020s in the same region. So, the global 2.85 ‰ decline in feather $\delta^{13}C$ values in this study (between the 1920s and the 2020s) could likely result from a change in phytoplankton productivity in the surrounding tropical marine ecosystems.

**Long-term trend in Hg contamination and its drivers**

Overall, our results (Table 1) are consistent with the range of average Hg concentrations observed for sooty terns elsewhere, such as in the Mozambique Channel (0.2 μg $g^{-1}$; Jaquemet et al., 2008; Kojadinovic et al., 2007), Pacific Islands (0.8 μg $g^{-1}$; Burger et al., 1992), the Seychelles (1.2 μg $g^{-1}$; Ramos and Tavares, 2010) and Puerto Rico (2.6 μg $g^{-1}$; Burger and Gochfeld, 1991). However, Ascension sooty terns exhibit Hg concentrations in the upper part of this range (1.5 μg $g^{-1}$). Among tropical seabirds, feather Hg values were intermediate compared with other sternids at other locations, such as brown noddies (*Anous stolidus*) in Hawaii (0.6 μg $g^{-1}$; Burger et al., 2001) and bridled terns (1.4 μg $g^{-1}$) and roseate terns (*Sterna dougallii*) in Puerto Rico (2.3 μg $g^{-1}$; Burger and Gochfeld, 1991). Low Hg contamination in sooty terns is consistent with their foraging ecology that largely depends on small epipelagic fish and invertebrates from surface waters (Ashmole, 1963a). Epipelagic prey exhibit lower Hg concentrations than mesopelagic and benthic prey (Chouvelon et al., 2012; Monteiro and Furness,

1997; Ochoa-Acuña et al., 2002), mainly because Hg methylation occurs in mesopelagic waters (Blum et al., 2013; Bowman et al., 2020; Cossa et al., 2009; Wang et al., 2018).

Few studies (n=14) have investigated long-term Hg trends in seabirds by using feathers as archives (Table S1). Most have focussed on temperate (*e.g.,* Appelquist et al., 1985; Thompson et al., 1993, 1992) and polar regions (*e.g.,* Bond et al., 2015; Carravieri et al., 2016; Scheifler et al., 2005). Only two have focussed on subtropical regions, in the Azores (Monteiro and Furness, 1997) and islands of the Pacific (Vo et al., 2011). Monteiro and Furness (1997) measured a 1.1% increase in Hg contamination *per* year between the 1880s and the 1990s in epipelagic Cory's shearwaters (*Calonectris borealis*) that share similar habitat with sooty terns, albeit in the North Atlantic Ocean. This was a stronger annual increase than that of 0.37% that we found if considering simply a linear trend. Despite different temporal coverage between studies, it appears that Hg transfer to predators has increased more slowly in the South than in the North Atlantic Ocean. Similar spatial disparities in Hg contamination were observed in tunas (Médieu et al., 2022), probably as a result of spatial differences in seawater Hg concentrations at the base of the food web, and inorganic Hg deposition among distinct oceanic regions. Mercury deposition could be higher in the subtropical than in the tropical Atlantic Ocean for two reasons. First, anthropogenic Hg was historically mainly emitted by industrialized countries from the Northern Hemisphere (Pacyna et al., 2006). Secondly, Hg is globally distributed by atmospheric circulation (Selin, 2009), which includes successive atmospheric circulation cells from the pole to the tropics, namely the Polar, the Ferrel and the Hadley Cells. As such, Hg emitted in Europe, for example, could be more easily deposited in the subtropical North Atlantic Ocean (*i.e.*, one circulation cell away) than in the tropical South Atlantic Ocean (*i.e.*, two circulation cells away).

Despite the temporal mismatch between feather Hg and stable isotopes (Bond, 2010), the trophic ecology of sooty terns influenced significantly their feather Hg contamination over time. Indeed, the best model explaining feather Hg contamination included both $\delta^{13}C$ and $\delta^{15}N$ values (Table 2), indicating that the temporal increase in feather Hg concentrations was associated with the strong decrease in $\delta^{13}C$ values and fluctuating $\delta^{15}N$ values observed over the past century (see **Discussion** above). However, the best model including both isotopic values explained only 14% of the total variation in Hg contamination, which suggests that other unknown factors (discussed below) also influenced long-term Hg contamination in sooty terns from Ascension Island. This is consistent with previous studies on other species (Bond et al., 2015; Carravieri et al., 2016; Vo et al., 2011). In addition, isotopic variations at the century scale are not simply or solely driven by changes in feeding habitat and trophic position, but likely by changes at the base of the food web, which are driven by several environmental and ecological processes (see previous section: «Long-term trend in foraging ecology: an update»). Therefore, our results suggest that the temporal trend in Hg transfer to predators in the South Atlantic Ocean was driven by trophic factors linked to ecosystem-wide changes, and other unknown factors. For instance, the increase in feather Hg concentrations observed from the 1920s to the 1970s was likely facilitated by growing Hg emissions during the Industrial Era with developing human activities, such as the Gold Rush, the burning of coal and intensifying manufacturing efforts to meet the military demands of World War II (Thompson et al., 1993). Between the 1970s and the 2000s, Hg concentrations appeared to stabilize. However, this phase included a very low number of available samples *per* year with high variability, implying large uncertainty in the generated models. Thus, whether Hg concentrations really remained stable between the 1970s and the 2000s is difficult to confirm. Mercury concentrations increased again from the 2000s to the present day, despite strong regulations restricting Hg emissions since the 1990s in the Northern

Hemisphere and 2017 globally (Minamata Convention on Mercury). This, together with other recently detected increases (e.g., Bond et al., 2015; Carravieri et al., 2016; Tartu et al., 2022), raises concerns for potential consequences on wildlife health.

**Did Hg drive sooty tern population collapse on Ascension Island?**

On Ascension Island, sooty terns suffered a 80% population collapse between the 1960s and the 1990s (Hughes et al., 2017). Reynolds et al. (2019) attributed this in part to a dietary shift from predominantly fish in the 1890s to the 1940s prior to the decline, to predominantly squid in the 1970s to the 2010s after it. With additional feather samples from the 2020s, our results revealed that isotopic niches were different between the two periods, with a significant difference in foraging habitat ($\delta^{13}C$) (agreeing with $\delta^{13}C$ values documented in Reynolds et al., 2019) but with an equivalent trophic position ($\delta^{15}N$) (Figure 2B).

Mercury concentrations were 38.8% higher post- compared to pre-population collapse (Figure 2A). These results are consistent with previous temporal comparisons, in which Hg concentrations have increased between historical and contemporary time periods in marine environments worldwide (Carravieri et al., 2016; Furness et al., 1995; Vo et al., 2011). During the period of population collapse, all Hg concentrations were relatively high with low variability, likely reflecting a generally high contamination in sooty terns. In comparison, there was more variability before and after the period of population collapse, probably because of slight differences in either diet or the proportions of different prey species constituting the diet. Given measured levels of Hg in sooty tern feathers − although elevated after the population collapse − it seems unlikely that Hg contamination drove the population decline of sooty terns on Ascension Island. Indeed, the extent of Hg contamination detected was below severe toxicity thresholds for seabird feathers (4-10 $\mu g.g^{-1}$; Ackerman et al., 2016; Chastel et al., 2022). Investigating

contamination by other pollutants (such as pesticides or plastics) would undoubtedly allow further insights into the risks and demographic stressors for this population, but our results reinforce the conclusions of Reynolds et al. (2019), that overharvesting of large predatory fish and climate change likely negatively impacted sooty tern trophic ecology, thereby resulting in elevated Hg contamination.

**Influence of climate change and fisheries on tropical Hg contamination**

Reynolds et al. (2019) highlighted the importance of increasing sea surface temperatures (SST) and tuna extraction by fisheries in explaining long-term changes in the trophic ecology of sooty terns breeding on Ascension Island. Sooty terns are heavily reliant on large schools of surface-swimming tunas, such as yellowfin (*Thunnus albacares*) and skipjack (*Katsuwonus pelamis*) tuna, to drive their common prey to the ocean surface, where many tropical seabirds forage in so-called « facilitated foraging » (Ashmole, 1963a; Au and Pitman, 1986; Ballance and Pitman, 1999; Maxwell and Morgan, 2013). Sooty terns are therefore susceptible to any over-exploitation and major declines in these associated species (Cullis-Suzuki and Pauly, 2010; Juan-Jordá et al., 2011). Nonetheless, under climate change, and specifically with changes in temperatures and salinity, global abundances of tunas are predicted to increase in tropical waters (Erauskin-Extramiana et al., 2019). Specifically, Ascension Island is predicted to become more suitable for several tuna species, including sooty tern associates (Townhill et al., 2021). Climate change and fishing pressure are therefore likely to impact Hg contamination in sooty terns, and hence in tropical marine ecosystems, even though the direction and the extent of these impacts are difficult to predict precisely.

Since seabird Hg contamination is heavily associated with their foraging ecology, climate change and fishing pressure also have indirect effects on Hg contamination through dietary

changes (prey switching), species' interactions and transfer through marine food webs (biotic factors). For example, MeHg concentrations increased in marine fish as a result of dietary shifts initiated by overfishing and with increasing SST (Schartup et al., 2019). Other environmental factors can also influence seabird Hg contamination, such as Hg transport, deposition, uptake and methylation rates in the ocean (Krabbenhoft and Sunderland, 2013). Mercury is mainly deposited in oceans by atmospheric fallouts (Eagles-Smith et al., 2018). Although Ascension Island is isolated, with its nearest neighbour, St Helena, located more than 1,300 km away, it is highly unlikely that Hg contamination results from local anthropogenic sources. As a volcanic island, Hg contamination might alternatively result from local geological activities, but there is no record of volcanic activity of Ascension Island over the last 500 to 1000 years (Preece et al., 2018). Instead, Hg contamination in sooty terns likely results from global Hg transport. In the ocean, sources of MeHg are multiple: methylation can occur in the sediments of continental shelves (Hammerschmidt and Fitzgerald, 2006) and estuaries (Heyes et al., 2006), within the water column (Cossa, 2013; Hammerschmidt and Bowman, 2012) and at deep-ocean hydrothermal vents (Bowman et al., 2016, 2015). Mercury methylated through these processes can then be widely distributed by ocean currents, both spatially (global ocean circulation) and vertically (vertical mixing and upwellings) (Mason et al., 2012). Climate change will likely influence all of these processes and could ultimately influence sooty tern contamination on different temporal and spatial scales. Methylation rate and bioavailability of Hg are also affected by other processes such as acidification, eutrophication and/or deoxygenation (Clayden et al., 2013; Gong et al., 2021; Jardine et al., 2013; Zhang et al., 2021). For instance, oxygen-depleted zones (*i.e.*, «dead zones») are increasing with climate change (Breitburg et al., 2018; Watson, 2016). Mercury methylation is substantially enhanced in low-oxygen zones in the ocean, that at low latitudes (*i.e.,* tropics) are the most vulnerable to further deoxygenation (Gruber, 2011). Tropical oceans should

thus be a priority for further studies of Hg contamination, especially in the context of climate change. Further research should focus on Hg stable isotopes to disentangle the different environmental and ecological factors involved, by identifying Hg sources and exploring the associated biogeochemical and trophic processes in the different compartments of tropical marine ecosystems (Renedo et al., 2020).

Mercury contamination of marine environments results from long-term processes, influenced by Hg transport, methylation and bioavailability, as well as from ecological interactions, both globally and locally. Undoubtedly, there is a time lag of years, decades, or even centuries between Hg emissions and deposition in the ocean and its resulting Hg contamination of marine food webs (Driscoll et al., 2013; Foster et al., 2019; Sunderland and Mason, 2007, UN Environment, 2018). Long-term monitoring of Hg is therefore crucial to: (i) assess the ongoing health status of tropical marine ecosystems and its variability over time; and (ii) ultimately minimize the risks of Hg exposure to wildlife and human populations alike, the latter relying heavily on marine food resources worldwide.

## ACKNOWLEDGMENTS

First, we thank all people involved in the original study of Reynolds et al. (2019), for bird sampling, both in museums and in the field. Funding for sample collections was provided by SJR. We are thankful to the Ascension Island Government for granting research permits to sample live birds in the 2000s, the 2010s and the 2020s. The authors are grateful to Carine Churlaud and Maud Brault-Favrou from the «Analyses Elémentaires» platform (LIENSs) for their support during Hg analysis and to Gaël Guillou from the «Analyses Isotopiques» platform (LIENSs) for running the stable isotope analyses. Special thanks are due to Sabrina Tartu and Céline Albert for statistical guidance during data exploration. We are grateful to Lucie Machin for the sooty tern drawing on the graphical abstract. Thanks are due to the CPER (Contrat de Projet Etat-Région) and the FEDER (Fonds Européen de Développement Régional) for funding the AMA and IRMS of LIENSs laboratory. The Institut Universitaire de France (IUF) is acknowledged for its support to PB as a Senior Member. This work benefitted from the French GDR "Aquatic Ecotoxicology"

framework, that aims to foster stimulating scientific discussions and collaborations for more integrative approaches.

The authors have no competing interest to declare.

**REFERENCES**


Ackerman, J.T., Eagles-Smith, C.A., Herzog, M.P., Hartman, C.A., Peterson, S.H., Evers, D.C., Jackson, A.K., Elliott, J.E., Vander Pol, S.S., Bryan, C.E., 2016. Avian mercury exposure and toxicological risk across western North America: A synthesis. Sci. Total Environ. 568, 749–769.

Albert, C., Renedo, M., Bustamante, P., Fort, J., 2019. Using blood and feathers to investigate large-scale Hg contamination in Arctic seabirds: A review. Environ. Res. 177, 108588.

Appelquist, H., Asbirk, S., Drabæk, I., 1984. Mercury monitoring: Mercury stability in bird feathers. Mar. Pollut. Bull. 15, 22–24.

Ashmole, N.P., 1963a. The biology of the Wideawake or sooty tern *Sterna Fuscata* on Ascension Island. Ibis 103b, 297–351.

Ashmole, N.P., 1963b. Molt and breeding in populations of the sooty tern *Sterna fuscata*. Postilla 76, 1–18.

Au, D.W.K., Pitman, R.L., 1986. Seabird interactions with dolphins and tuna in the eastern tropical Pacific. The Condor 88, 304–317.

Barton (2022). MuMIn: Multi-Model Inference. R package version 1.46.0. https://CRAN.R-project.org/package=MuMIn

Blum, J.D., Popp, B.N., Drazen, J.C., Anela Choy, C., Johnson, M.W., 2013. Methylmercury production below the mixed layer in the North Pacific Ocean. Nat. Geosci. 6, 879–884.

Bond, A.L., 2010. Relationships between stable isotopes and metal contaminants in feathers are spurious and biologically uninformative. Environ. Pollut. 158, 1182–1184.

Bond, A.L., Diamond, A.W., 2009. Total and methyl mercury concentrations in seabird feathers and eggs. Arch. Environ. Contam. Toxicol. 56, 286–291.

Bond, A.L., Hobson, K.A., Branfireun, B.A., 2015. Rapidly increasing methyl mercury in endangered ivory gull (*Pagophila eburnea*) feathers over a 130 year record. Proc. Biol. Sci. 282, 1–8.

Bowman, K.L., Hammerschmidt, C.R., Lamborg, C.H., Swarr, G., 2015. Mercury in the North Atlantic Ocean: The U.S. GEOTRACES zonal and meridional sections. Deep Sea Res. Part II Top. Stud. Oceanogr., GEOTRACES GA-03 - The U.S. GEOTRACES North Atlantic Transect 116, 251–261.

Bowman, K.L., Hammerschmidt, C.R., Lamborg, C.H., Swarr, G.J., Agather, A.M., 2016. Distribution of mercury species across a zonal section of the eastern tropical South Pacific Ocean (U.S. GEOTRACES GP16). Mar. Chem. 186, 156–166.

Bowman, K.L., Lamborg, C.H., Agather, A.M., 2020. A global perspective on mercury cycling in the ocean. Sci. Total Environ. 710, 136166.

Breitburg, D., Levin, L.A., Oschlies, A., Grégoire, M., Chavez, F.P., Conley, D.J., Garçon, V., Gilbert, D., Gutiérrez, D., Isensee, K., Jacinto, G.S., Limburg, K.E., Montes, I., Naqvi, S.W.A., Pitcher, G.C., Rabalais, N.N., Roman, M.R., Rose, K.A., Seibel, B.A., Telszewski, M., Yasuhara, M., Zhang, J., 2018. Declining oxygen in the global ocean and coastal waters. Science 359, eaam7240.

Burger, J., Gochfeld, M., 2004. Marine birds as sentinels of environmental pollution. EcoHealth 1, 263–274.

Burger, J., Gochfeld, M., 1991. Lead, mercury, and cadmium in feathers of tropical terns in Puerto Rico and Australia. Arch. Environ. Contam. Toxicol. 21, 311–315.

Burger, J., Schreiber, E.A.E., Gochfeld, M., 1992. Lead, cadmium, selenium and mercury in seabird feathers from the tropical mid-pacific. Environ. Toxicol. Chem. 11, 815–822.

Burger, J., Shukla, T., Dixon, C., Shukla, S., McMahon, M.J., Ramos, R., Gochfeld, M., 2001. Metals in feathers of sooty tern, white tern, gray-backed tern, and brown noddy from Islands in the North Pacific. Environ. Monit. Assess. 71, 71–89.

Burnham, K.P., Anderson, D.R., 2002. Model selection and multimodel inference: A practical information - Theoretic approach, 2nd ed. Springer US.

Carravieri, A., Bustamante, P., Churlaud, C., Fromant, A., Cherel, Y., 2014. Moulting patterns drive within-individual variations of stable isotopes and mercury in seabird body feathers: implications for monitoring of the marine environment. Mar. Biol. 161, 963–968.

Carravieri, A., Cherel, Y., Jaeger, A., Churlaud, C., Bustamante, P., 2016. Penguins as bioindicators of mercury contamination in the southern Indian Ocean: geographical and temporal trends. Environ. Pollut. Barking Essex 1987 213, 195–205.

Chastel, O., Fort, J., Ackerman, J.T., Albert, C., Angelier, F., Basu, N., Blévin, P., Brault-Favrou, M., Bustnes, J.O., Bustamante, P., Danielsen, J., Descamps, S., Dietz, R., Erikstad, K.E., Eulaers, I., Ezhov, A., Fleishman, A.B., Gabrielsen, G.W., Gavrilo, M., Gilchrist, G., Gilg, O., Gíslason, S., Golubova, E., Goutte, A., Grémillet, D., Hallgrimsson, G.T., Hansen, E.S., Hanssen, S.A., Hatch, S., Huffeldt, N.P., Jakubas, D., Jónsson, J.E., Kitaysky, A.S., Kolbeinsson, Y., Krasnov, Y., Letcher, R.J., Linnebjerg, J.F., Mallory, M., Merkel, F.R., Moe, B., Montevecchi, W.J., Mosbech, A., Olsen, B., Orben, R.A., Provencher, J.F., Ragnarsdottir, S.B., Reiertsen, T.K., Rojek, N., Romano, M., Søndergaard, J., Strøm, H., Takahashi, A., Tartu, S., Thórarinsson, T.L., Thiebot, J.-B., Will, A.P., Wilson, S., Wojczulanis-Jakubas, K., Yannic, G., 2022. Mercury contamination and potential health risks to Arctic seabirds and shorebirds. Sci. Total Environ. 156944.

Cherel, Y., Barbraud, C., Lahournat, M., Jaeger, A., Jaquemet, S., Wanless, R.M., Phillips, R.A., Thompson, D.R., Bustamante, P., 2018. Accumulate or eliminate? Seasonal mercury dynamics in albatrosses, the most contaminated family of birds. Environ. Pollut. 241, 124–135.

Cherel, Y., Connan, M., Jaeger, A., Richard, P., 2014. Seabird year-round and historical feeding ecology: blood and feather $\delta^{13}C$ and $\delta^{15}N$ values document foraging plasticity of small sympatric petrels. Mar. Ecol. Prog. Ser. 505, 267–280.

Chouvelon, T., Spitz, J., Caurant, F., Mèndez-Fernandez, P., Autier, J., Lassus-Débat, A., Chappuis, A., Bustamante, P., 2012. Enhanced bioaccumulation of mercury in deep-sea fauna from the Bay of Biscay (north-east Atlantic) in relation to trophic positions identified by analysis of carbon and nitrogen stable isotopes. Deep Sea Res. Part Oceanogr. Res. Pap. 65, 113–124.

Choy, E.S., Blight, L.K., Elliott, J.E., Hobson, K.A., Zanuttig, M., Elliott, K.H., 2022. Stable mercury trends support a long-term diet shift away from marine foraging in Salish Sea glaucous-winged gulls over the last century. Environ. Sci. Technol. 56, 12097–12105.

Cifuentes, L.A., Sharp, J.H., Fogel, M.L., 1988. Stable carbon and nitrogen isotope biogeochemistry in the Delaware estuary. Limnol. Oceanogr. 33, 1102–1115.

Clayden, M.G., Kidd, K.A., Wyn, B., Kirk, J.L., Muir, D.C.G., O'Driscoll, N.J., 2013. Mercury biomagnification through food webs is affected by physical and chemical characteristics of lakes. Environ. Sci. Technol. 47, 12047–12053.

Cossa, D., 2013. Methylmercury manufacture. Nat. Geosci. 6, 810–811. https://doi.org/10.1038/ngeo1967

Cossa, D., Averty, B., Pirrone, N., 2009. The origin of methylmercury in open Mediterranean waters. Limnol. Oceanogr. 54, 837–844.

Crewther, W.G., Fraser, R.D., Lennox, F.G., Lindley, H., 1965. The chemistry of keratins. Adv. Protein Chem. 20, 191–346.

DeNiro, M.J., Epstein, S., 1978. Influence of diet on the distribution of carbon isotopes in animals. Geochim. Cosmochim. Acta 42, 495–506.

Driscoll, C.T., Mason, R.P., Chan, H.M., Jacob, D.J., Pirrone, N., 2013. Mercury as a global pollutant: Sources, pathways, and effects. Environ. Sci. Technol. 47, 4967–4983.

Eagles-Smith, C.A., Silbergeld, E.K., Basu, N., Bustamante, P., Diaz-Barriga, F., Hopkins, W.A., Kidd, K.A., Nyland, J.F., 2018. Modulators of mercury risk to wildlife and humans in the context of rapid global change. Ambio 47, 170–197.

Eide, M., Olsen, A., Ninnemann, U.S., Eldevik, T., 2017. A global estimate of the full oceanic $^{13}C$ Suess effect since the preindustrial. Glob. Biogeochem. Cycles 31, 492–514.

Fort, J., Grémillet, D., Traisnel, G., Amélineau, F., Bustamante, P., 2016. Does temporal variation of mercury levels in Arctic seabirds reflect changes in global environmental contamination, or a modification of Arctic marine food web functioning? Environ. Pollut. 211, 382–388.

Foster, K.L., Braune, B.M., Gaston, A.J., Mallory, M.L., 2019. Climate influence on mercury in Arctic seabirds. Sci. Total Environ. 693, 133569.

France, R., 1995. Carbon-13 enrichment in benthic compared to planktonic algae: Foodweb implications. Mar. Ecol. Prog. Ser. 124, 307–312.

Furness, R.W., 1993. Birds as monitors of pollutants, in: Furness, R.W., Greenwood, J.J.D. (Eds.), Birds as Monitors of Environmental Change. Springer Netherlands, Dordrecht, pp. 86–143.

Furness, R.W., Camphuysen, K. (C J.), 1997. Seabirds as monitors of the marine environment. ICES J. Mar. Sci. 54, 726–737.

Furness, R.W., Thompson, D.R., Becker, P.H., 1995. Spatial and temporal variation in mercury contamination of seabirds in the North Sea. Helgoländer Meeresunters. 49, 605–615.

Goering, J., Alexander, V., Haubenstock, N., 1990. Seasonal variability of stable carbon and nitrogen isotope ratios of organisms in a North Pacific Bay. Estuar. Coast. Shelf Sci. 30, 239–260.

Gong, H., Li, C., Zhou, Y., 2021. Emerging global ocean deoxygenation across the 21$^{st}$ century. Geophys. Res. Lett. 48, e2021GL095370.

Gruber, N., 2011. Warming up, turning sour, losing breath: ocean biogeochemistry under global change. Philos. Trans. R. Soc. Math. Phys. Eng. Sci. 369, 1980–1996.

Hammerschmidt, C.R., Bowman, K.L., 2012. Vertical methylmercury distribution in the subtropical North Pacific Ocean. Mar. Chem. 132–133, 77–82.

Hammerschmidt, C.R., Fitzgerald, W.F., 2006. Methylmercury cycling in sediments on the continental shelf of southern New England. Geochim. Cosmochim. Acta 70, 918–930.

Heyes, A., Mason, R.P., Kim, E.-H., Sunderland, E., 2006. Mercury methylation in estuaries: Insights from using measuring rates using stable mercury isotopes. Mar. Chem., 8th International Estuarine Biogeochemistry Symposium - Introduction 102, 134–147.

Hilton, G.M., Thompson, D.R., Sagar, P.M., Cuthbert, R.J., Cherel, Y., Bury, S.J., 2006. A stable isotopic investigation into the causes of decline in a sub-Antarctic predator, the rockhopper penguin Eudyptes chrysocome. Glob. Change Biol. 12, 611–625.

Hirons, A.C., Schell, D.M., Finney, B.P., 2001. Temporal records of $\delta^{13}C$ and $\delta^{15}N$ in North Pacific pinnipeds: Inferences regarding environmental change and diet. Oecologia 129, 591–601.

Hobson, K.A., 1999. Tracing origins and migration of wildlife using stable isotopes: A review. Oecologia 120, 314–326.

Hogstad, O., Nygård, T., Gätzschmann, P., Lierhagen, S., Thingstad, P.G., 2003. Bird skins in museum collections: Are they suitable as indicators of environmental metal load after conservation procedures? Environ. Monit. Assess. 87, 47–56.

Honda, K., Nasu, T., Tatsukawa, R., 1986. Seasonal changes in mercury accumulation in the black-eared kite, *Milvus migrans lineatus*. Environ. Pollut. Ser. Ecol. Biol. 42, 325–334.

Horowitz, H.M., Jacob, D.J., Zhang, Y., Dibble, T.S., Slemr, F., Amos, H.M., Schmidt, J.A., Corbitt, E.S., Marais, E.A., Sunderland, E.M., 2017. A new mechanism for atmospheric mercury redox chemistry: Implications for the global mercury budget. Atmospheric Chem. Phys. 17, 6353–6371.

Hughes, B.J., Martin, G.R., Giles, A.D., Reynolds, S.J., 2017. Long-term population trends of Sooty Terns *Onychoprion fuscatus*: Implications for conservation status. Popul. Ecol. 59, 213–224.

Hughes, B.J., Martin, G.R., Reynolds, S.J., 2012. Estimate of Sooty Tern *Onychoprion fuscatus* population size following cat eradication on Ascension Island, central Atlantic. Bull ABC 19, 166–171.

Jaeger, A., Blanchard, P., Richard, P., Cherel, Y., 2009. Using carbon and nitrogen isotopic values of body feathers to infer inter- and intra-individual variations of seabird feeding ecology during moult. Mar. Biol. 156, 1233–1240.

Jaeger, A., Cherel, Y., 2011. Isotopic investigation of contemporary and historic changes in penguin trophic niches and carrying capacity of the Southern Indian Ocean. PLOS ONE 6, e16484.

Jaquemet, S., Potier, M., Cherel, Y., Kojadinovic, J., Bustamante, P., Richard, P., Catry, T., Ramos, J.A., Le Corre, M., 2008. Comparative foraging ecology and ecological niche of a superabundant tropical seabird: the sooty tern *Sterna fuscata* in the southwest Indian Ocean. Mar. Biol. 155, 505–520.

Jardine, T.D., Kidd, K.A., O' Driscoll, N., 2013. Food web analysis reveals effects of pH on mercury bioaccumulation at multiple trophic levels in streams. Aquat. Toxicol. 132–133, 46–52.

Jarek, S., 2012. mvnormtest: Normality test for multivariate variables. R package version 0.1-9. https://CRAN.R-project.org/package=mvnormtest

Johnson, J.B., Omland, K.S., 2004. Model selection in ecology and evolution. Trends Ecol. Evol. 19, 101–108.

Juan-Jordá, M.J., Mosqueira, I., Cooper, A.B., Freire, J., Dulvy, N.K., 2011. Global population trajectories of tunas and their relatives. Proc. Natl. Acad. Sci. 108, 20650–20655.

Keeling, C.D., 1979. The Suess effect: $^{13}$Carbon-$^{14}$Carbon interrelations. Environ. Int. 2, 229–300.

Kelly, J.F., 2000. Stable isotopes of carbon and nitrogen in the study of avian and mammalian trophic ecology. Can. J. Zool. 78, 1–27.

Kojadinovic, J., Bustamante, P., Churlaud, C., Cosson, R.P., Le Corre, M., 2007. Mercury in seabird feathers: Insight on dietary habits and evidence for exposure levels in the western Indian Ocean. Sci. Total Environ. 384, 194–204.

Körtzinger, A., Quay, P.D., Sonnerup, R.E., 2003. Relationship between anthropogenic $CO_2$ and the $^{13}$C Suess effect in the North Atlantic Ocean. Glob. Biogeochem. Cycles 17, 5-1-5–20.

Krabbenhoft, D.P., Sunderland, E.M., 2013. Global change and mercury. Science 341, 1457–1458.

Lamborg, C.H., Hammerschmidt, C.R., Bowman, K.L., Swarr, G.J., Munson, K.M., Ohnemus, D.C., Lam, P.J., Heimbürger, L.-E., Rijkenberg, M.J.A., Saito, M.A., 2014. A global ocean inventory of anthropogenic mercury based on water column measurements. Nature 512, 65–68.

Lorrain, A., Pethybridge, H., Cassar, N., Receveur, A., Allain, V., Bodin, N., Bopp, L., Choy, C.A., Duffy, L., Fry, B., Goñi, N., Graham, B.S., Hobday, A.J., Logan, J.M., Ménard, F., Menkes, C.E., Olson, R.J., Pagendam, D.E., Point, D., Revill, A.T., Somes, C.J., Young, J.W., 2020. Trends in tuna carbon isotopes suggest global changes in pelagic phytoplankton communities. Glob. Change Biol. 26, 458–470.

Mason, R.P., Choi, A.L., Fitzgerald, W.F., Hammerschmidt, C.R., Lamborg, C.H., Soerensen, A.L., Sunderland, E.M., 2012. Mercury biogeochemical cycling in the ocean and policy implications. Environ. Res. 119, 101–117.

Maxwell, S.M., Morgan, L.E., 2013. Foraging of seabirds on pelagic fishes: Implications for management of pelagic marine protected areas. Mar. Ecol. Prog. Ser. 481, 289–303.

McMahon, K.W., Hamady, L.L., Thorrold, S.R., 2013. Ocean ecogeochemistry: A review. Oceanogr. Mar. Biol. Annu. Rev. 51, 327–374.

McMahon, K.W., Newsome, S.D., 2019. Chapter 7 - Amino acid isotope analysis: A new frontier in studies of animal migration and foraging ecology, in: Hobson, K.A., Wassenaar, L.I. (Eds.), Tracking Animal Migration with Stable Isotopes (Second Edition). Academic Press, pp. 173–190.

Médieu, A., Point, D., Itai, T., Angot, H., Buchanan, P.J., Allain, V., Fuller, L., Griffiths, S., Gillikin, D.P., Sonke, J.E., Heimbürger-Boavida, L.-E., Desgranges, M.-M., Menkes, C.E., Madigan, D.J., Brosset, P., Gauthier, O., Tagliabue, A., Bopp, L., Verheyden, A., Lorrain, A., 2022. Evidence that Pacific tuna mercury levels are driven by marine methylmercury production and anthropogenic inputs. Proc. Natl. Acad. Sci. 119, e2113032119.

Monteiro, L.R., Furness, R.W., 1997. Accelerated increase in mercury contamination in north Atlantic mesopelagic food chains as indicated by time series of seabird feathers. Environ. Toxicol. Chem. 16, 2489–2493.

Ochoa-Acuña, H., Sepúlveda, M.S., Gross, T.S., 2002. Mercury in feathers from Chilean birds: Influence of location, feeding strategy, and taxonomic affiliation. Mar. Pollut. Bull. 44, 340–345.

O'Reilly, C.M., Alin, S.R., Plisnier, P.-D., Cohen, A.S., McKee, B.A., 2003. Climate change decreases aquatic ecosystem productivity of Lake Tanganyika, Africa. Nature 424, 766–768.

Ostrom, N.E., Macko, S.A., Deibel, D., Thompson, R.J., 1997. Seasonal variation in the stable carbon and nitrogen isotope biogeochemistry of a coastal cold ocean environment. Geochim. Cosmochim. Acta 61, 2929–2942.

Pacyna, E.G., Pacyna, J.M., Steenhuisen, F., Wilson, S., 2006. Global anthropogenic mercury emission inventory for 2000. Atmos. Environ. 40, 4048–4063.

Piatt, J.F., Harding, A.M.A., Shultz, M., Speckman, S.G., Pelt, T.I. van, Drew, G.S., Kettle, A.B., 2007. Seabirds as indicators of marine food supplies: Cairns revisited. Mar. Ecol. Prog. Ser. 352, 221–234.

Pinheiro J., Bates D., DebRoy S., Sarkar D., R Core Team, 2020. nlme: Linear and nonlinear mixed effects models. R package version 3.1-149, https://CRAN.R-project.org/package=nlme

Preece, K., Mark, D.F., Barclay, J., Cohen, B.E., Chamberlain, K.J., Jowitt, C., Vye-Brown, C., Brown, R.J., Hamilton, S., 2018. Bridging the gap: 40Ar/39Ar dating of volcanic eruptions from the 'Age of Discovery.' Geology 46, 1035–1038.

Quillfeldt, P., Masello, J.F., McGill, R.A., Adams, M., Furness, R.W., 2010. Moving polewards in winter: a recent change in the migratory strategy of a pelagic seabird? Front. Zool. 7, 15.

R Core Team, 2020. R: A language and environment for statistical computing. R Foundation for Statistical Computing, Vienna, Austria. URL https://www.R-project.org/

Ramos, J.A., Tavares, P.C., 2010. Mercury levels in the feathers of breeding seabirds in the Seychelles, western Indian Ocean, from 1996 to 2005. Emu - Austral Ornithol. 110, 87–91.

Rau, G.H., Takahashi, T., Des Marais, D.J., Repeta, D.J., Martin, J.H., 1992. The relationship between $\delta^{13}C$ of organic matter and $[CO_2(aq)]$ in ocean surface water: Data from a JGOFS site in the northeast Atlantic Ocean and a model. Geochim. Cosmochim. Acta 56, 1413–1419.

Renedo, M., Amouroux, D., Albert, C., Bérail, S., Br\aathen, V.S., Gavrilo, M., Grémillet, D., Helgason, H.H., Jakubas, D., Mosbech, A., Strøm, H., Tessier, E., Wojczulanis-Jakubas, K., Bustamante, P., Fort, J., 2020. Contrasting spatial and seasonal trends of methylmercury exposure pathways of Arctic seabirds: Combination of large-scale tracking and stable isotopic approaches. Environ. Sci. Technol. 54, 13619–13629.

Renedo, M., Amouroux, D., Pedrero, Z., Bustamante, P., Cherel, Y., 2018. Identification of sources and bioaccumulation pathways of MeHg in subantarctic penguins: A stable isotopic investigation. Sci. Rep. 8(1): 8865.

Renedo, M., Bustamante, P., Tessier, E., Pedrero, Z., Cherel, Y., Amouroux, D., 2017. Assessment of mercury speciation in feathers using species-specific isotope dilution analysis. Talanta 174, 100–110.

Reynolds, S.J., Hughes, B.J., Wearn, C.P., Dickey, R.C., Brown, J., Weber, N.L., Weber, S.B., Paiva, V.H., Ramos, J.A., 2019. Long-term dietary shift and population decline of a pelagic seabird—A health check on the tropical Atlantic? Glob. Change Biol. 25, 1383–1394.

Reynolds, S.J., Martin, G.R., Dawson, A., Wearn, C.P., Hughes, B.J., 2014. The sub-annual breeding cycle of a tropical seabird. PLoS ONE 9, e93582.

Reynolds, S.J., Wearn, C.P., Hughes, B.J., Dickey, R.C., Garrett, L.J.H., Walls, S., Hughes, F.T., Weber, N., Weber, S.B., Leat, E.H.K., Andrews, K., Ramos, J.A., Paiva, V.H., 2021. Year-round movements of sooty terns (*Onychoprion fuscatus*) nesting within one of the Atlantic's largest Marine Protected Areas. Front. Mar. Sci. 8, 744506.

Sackett, W.M., Eckelmann, W.R., Bender, M.L., Bé, A.W.H., 1965. Temperature dependence of carbon isotope composition in marine plankton and sediments. Science 148, 235–237.

Schartup, A.T., Thackray, C.P., Qureshi, A., Dassuncao, C., Gillespie, K., Hanke, A., Sunderland, E.M., 2019. Climate change and overfishing increase neurotoxicant in marine predators. Nature 572, 648–650.

Schell, D.M., 2000. Declining carrying capacity in the Bering Sea: Isotopic evidence from whale baleen. Limnol. Oceanogr. 45, 459–462.

Selin, N.E., 2009. Global biogeochemical cycling of mercury: A review. Annu. Rev. Environ. Resour. 34, 43–63.

Streets, D.G., Horowitz, H.M., Lu, Z., Levin, L., Thackray, C.P., Sunderland, E.M., 2019. Five hundred years of anthropogenic mercury: Spatial and temporal release profiles. Environ. Res. Lett. 14(8): 084004.

Sunderland, E.M., Krabbenhoft, D.P., Moreau, J.W., Strode, S.A., Landing, W.M., 2009. Mercury sources, distribution, and bioavailability in the North Pacific Ocean: Insights from data and models. Glob. Biogeochem. Cycles 23(2), GB2010.

Sunderland, E.M., Mason, R.P., 2007. Human impacts on open ocean mercury concentrations. Glob. Biogeochem. Cycles 21(4), GB4022.

Takeuchi, T., Morikawa, N., Matsumoto, H., Shiraishi, Y., 1962. A pathological study of Minamata disease in Japan. Acta Neuropathol. (Berl.) 2, 40–57.

Tartu, S., Blévin, P., Bustamante, P., Angelier, F., Bech, C., Bustnes, J.O., Chierici, M., Fransson, A., Gabrielsen, G.W., Goutte, A., Moe, B., Sauser, C., Sire, J., Barbraud, C., Chastel, O., 2022. A U-Turn for mercury concentrations over 20 years: How do environmental conditions affect exposure in Arctic seabirds? Environ. Sci. Technol. 56, 2443–2454.

Thompson, D.R., Bearhop, S., Speakman, J.R., Furness, R.W., 1998. Feathers as a means of monitoring mercury in seabirds: Insights from stable isotope analysis. Environ. Pollut. 101, 193–200.

Thompson, D.R., Becker, P.H., Furness, R.W., 1993. Long-term changes in mercury concentrations in Herring Gulls *Larus argentatus* and Common Terns *Sterna hirundo* from the German North Sea Coast. J. Appl. Ecol. 30, 316–320.

Thompson, D.R., Furness, R.W., 1989. Comparison of the levels of total and organic mercury in seabird feathers. Mar. Pollut. Bull. 20, 577–579.

Thompson, D.R., Furness, R.W., Walsh, P.M., 1992. Historical changes in mercury concentrations in the marine ecosystem of the North and North-East Atlantic Ocean as indicated by seabird feathers. J. Appl. Ecol. 29, 79–84.

Townhill, B.L., Couce, E., Bell, J., Reeves, S., Yates, O., 2021. Climate change impacts on Atlantic oceanic island tuna fisheries. Front. Mar. Sci. 8.

UN Environment (2019). Global Mercury Assessment 2018. UN Environment Programme, Chemicals and Health Branch, Geneva, Switzerland

Vizzini, S., Mazzola, A., 2003. Seasonal variations in the stable carbon and nitrogen isotope ratios ($^{13}C/^{12}C$ and $^{15}N/^{14}N$) of primary producers and consumers in a western Mediterranean coastal lagoon. Mar. Biol. 142, 1009–1018.

Vo, A.-T.E., Bank, M.S., Shine, J.P., Edwards, S.V., 2011. Temporal increase in organic mercury in an endangered pelagic seabird assessed by century-old museum specimens. Proc. Natl. Acad. Sci. 108, 7466–7471.

Wang, K., Munson, K.M., Beaupré-Laperrière, A., Mucci, A., Macdonald, R.W., Wang, F., 2018. Subsurface seawater methylmercury maximum explains biotic mercury concentrations in the Canadian Arctic. Sci. Rep. 8, 1–5.

Watson, A.J., 2016. Oceans on the edge of anoxia. Science 354, 1529–1530.

Wood, S.N., 2011. Fast stable restricted maximum likelihood and marginal likelihood estimation of semiparametric generalized linear models. J. R. Stat. Soc. Ser. B Stat. Methodol. 73, 3–36.

Zhang, Y., Dutkiewicz, S., Sunderland, E.M., 2021. Impacts of climate change on methylmercury formation and bioaccumulation in the 21st century ocean. One Earth 4, 279–288.

Zeileis, A., Hothorn, T., 2002. Diagnostic Checking in Regression Relationships. R News 2(3), 7-10. https://CRAN.R-project.org/doc/Rnews/

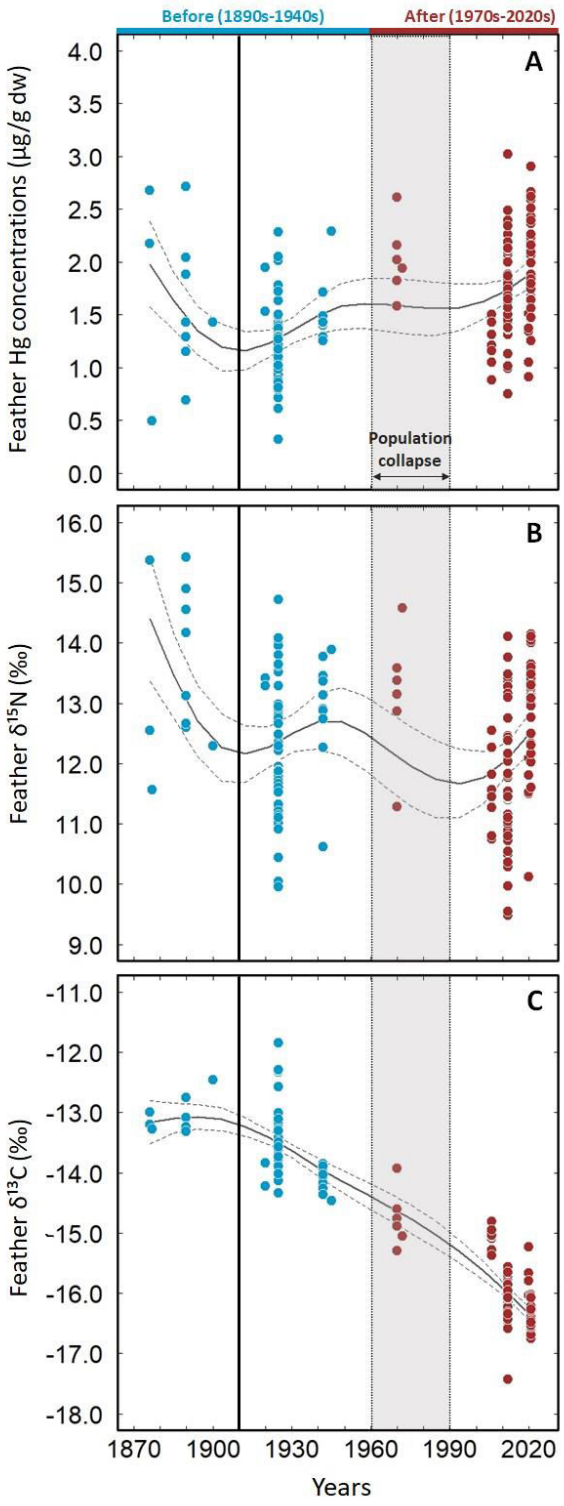


**Figure 1.** Long-term trends in **(A)** feather Hg concentrations, **(B)** nitrogen ($\delta^{15}N$) and **(C)** carbon ($\delta^{13}C$) isotopic values of sooty terns breeding on Ascension Island (South Atlantic Ocean) between 1876 and 2021 (*i.e.*, over 145 years). The $\delta^{13}C$ values are corrected for the Suess Effect and phytoplankton fractionation (cf. details in **Materials and Methods**). The grey area represents the transition between the period before (blue) and after (red) population collapse that occurred between the 1960s and the 1990s (see Reynolds et al., 2019 for further details). Solid and dotted lines represent the best-fitting model detected from construction of GAMs and the confidence interval, respectively. To the right of the vertical solid line at 1910 is the period of realistic interpretation (see **Material and Methods** and **Discussion** for further details).

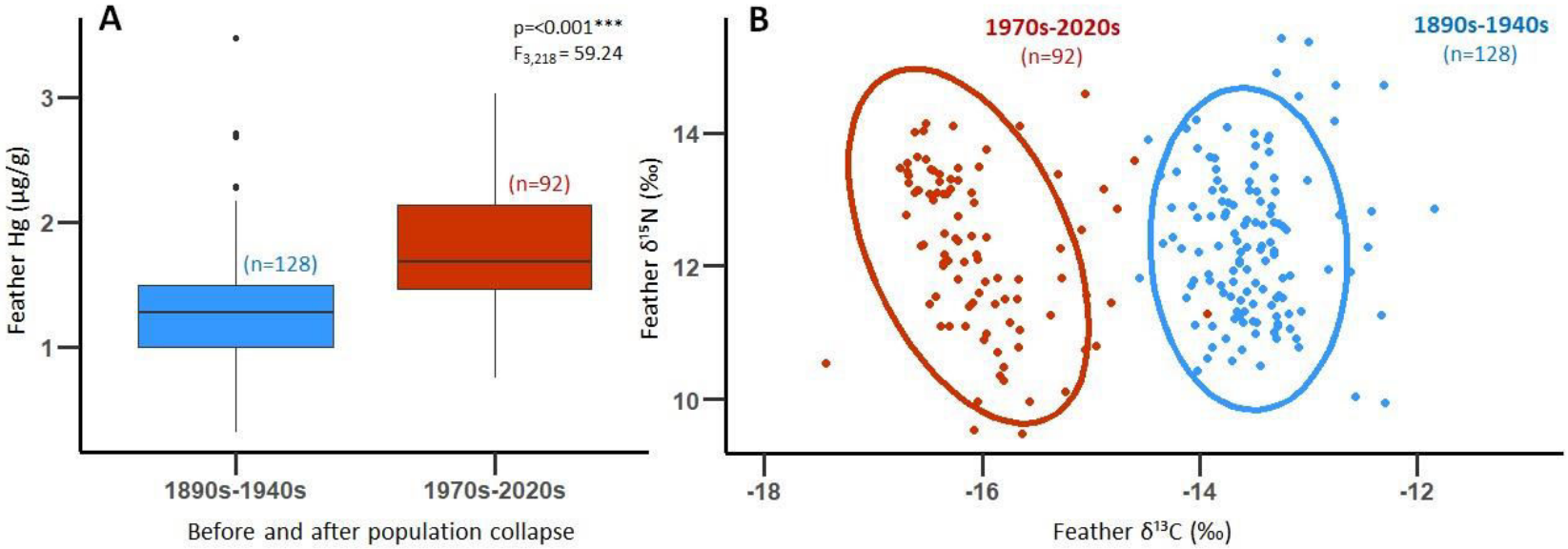


**Figure 2.** Difference in **(A)** Hg concentrations and **(B)** isotopic niches ($\delta^{13}C$ and $\delta^{15}N$ values) from feathers of adult sooty terns relative to the population collapse on Ascension Island between the 1960s and the 1990s. Points, ellipses (including 90% of the data) and bars in blue and red are before (n=128) and after (n=92) the population collapse, respectively. n indicates the sample sizes. Boxplots indicate median values (midlines), errors bars (whiskers) and outliers (black dots).

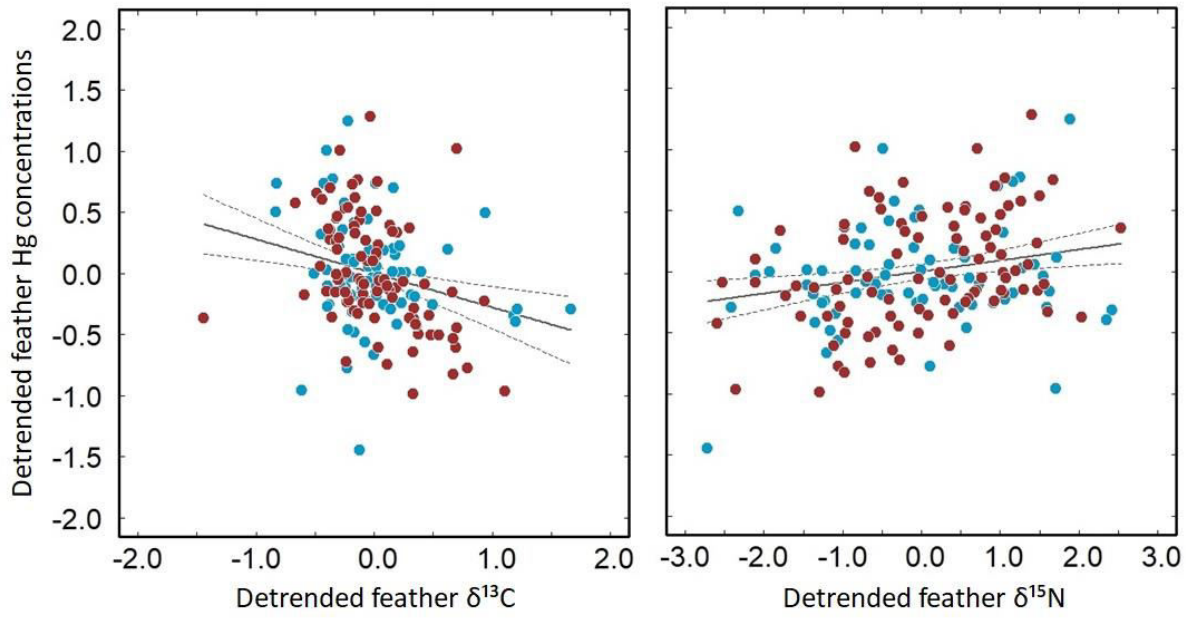


**Figure 3.** Relationship between time-detrended Hg concentrations and time-detrended stable isotope values in feathers of adult sooty terns breeding on Ascension Island in the South Atlantic Ocean between 1876 and 2021 (*i.e.,* over 145 years). The tern population collapsed between the 1960s and the 1990s (see Reynolds et al., 2019 for further details), with data before- (in blue) and after (in red) the collapse. All data were scaled. Solid and dashed lines represent the best-fitting linear model and the 95% confidence interval, respectively.

**Table 1.** Mercury concentrations and stable isotope values (mean ± SD, range) in feathers of sooty terns (n=220) breeding on Ascension Island (South Atlantic Ocean) from the 1870s to the 2020s, before (1840s-1940s) and after (1970s-2020s) their population collapse. Total-Hg (THg) was measured in all samples, whereas methyl-Hg (MeHg) was analysed when inorganic contamination by museum preservatives was detected (*i.e.,* prior to the 1970s). Feather $\delta^{13}C$ (corrected for the Suess Effect) and $\delta^{15}N$ values are proxies for the foraging habitat and trophic position during moult, respectively. n indicates sample size for each decade or period.

| Decade | n | Feather THg (µg $g^{-1}$) | Feather MeHg (µg $g^{-1}$) | Corrected feather $\delta^{13}C$ (‰) | Feather $\delta^{15}N$ (‰) |
|---|---|---|---|---|---|
| 1890 | 11 | 70.12 ± 87.34 (1.65 – 264.92) | 1.63 ± 0.74 (0.49 – 2.71) | -13.11 ± 0.27 (-13.32, -12.46) | 13.56 ± 1.36 (11.57 – 15.42) |
| 1920 | 107 | 5.25 ± 7.82 (1.65 – 55.57) | 1.24 ± 0.42 (0.32 – 3.47) | -13.50 ± 0.45 (-14.55, -11.85) | 12.15 ± 1.04 (9.96 – 14.72) |
| 1940 | 10 | 9.70 ± 7.51 (3.36 – 26.12) | 1.51 ± 0.30 (1.25 – 2.29) | -14.10 ± 0.21 (-14.47, -13.85) | 12.90 ± 0.94 (10.61 – 13.89) |
| 1970 | 6 | 5.25 ± 6.50 (2.20 – 18.51) | 2.02 ± 0.35 (1.58 – 2.61) | -14.76 ± 0.47 (-15.30, -13.93) | 13.14 ± 1.08 (11.28 – 14.58) |
| 2000 | 8 | 1.21 ± 0.20 (0.88 – 1.50) | - | -15.11 ± 0.19 (-15.37, -14.81) | 11.56 ± 0.64 (10.74 – 12.55) |
| 2010 | 44 | 1.72 ± 0.43 (0.75 – 3.02) | - | -16.11 ± 0.33 (-17.44, -15.56) | 11.75 ± 1.19 (9.49 – 14.11) |
| 2020 | 34 | 1.97 ± 0.49 (0.91 – 2.90) | - | -16.35 ± 0.35 (-16.75, -15.23) | 12.89 ± 0.89 (10.12-14.14) |
| **1890-1940** | **128** | - | 1.29 ± 0.46 (0.32 – 3.47) | -13.51 ± 0.47 (-14.55, -11.85) | 12.33 ± 1.13 (9.96 – 15.42) |
| **1970-2020** | **92** | 1.79 ± 0.48 (0.75 – 3.02) | - | -16.02 ± 0.58 (-17.44, -13.93) | 12.24 ± 1.19 (9.49 – 14.58) |

**Table 2.** AICc model ranking from statistical analyses of feather Hg concentrations from sooty terns breeding on Ascension Island. Models are Generalized Additive Models (GAMs) with a Gaussian distribution and an identity link function. Variables were all time-detrended (cf. **Materials and Methods**). Abbreviations: k: number of parameters; $AIC_c$: Aikaike's Information Criterion adjusted for small sample size; $w_i$: $AIC_c$ weights.

| Models | k | $AIC_c$ | $\Delta AIC_c$ [a] | $w_i$ [b] |
|---|---|---|---|---|
| **Detrended $\delta^{13}C$ + Detrended $\delta^{15}N$** | **4** | **184.52** | **0.00** | **0.96** |
| Detrended $\delta^{13}C$ | 3 | 191.49 | 6.97 | 0.03 |
| Detrended $\delta^{15}N$ | 3 | 193.75 | 9.23 | 0.01 |
| NULL | 2 | 206.61 | 22.09 | 0.00 |

[a]A model with $\Delta AIC_c = 0$ is interpreted as the best model among all the selected ones (in bold).

[b]Weights are cumulative (sum to 1).

Supplementary Material

# A century of mercury: Ecosystem-wide changes drive increasing contamination of a tropical seabird species in the South Atlantic Ocean

*Fanny Cusset, S. James Reynolds, Alice Carravieri, David Amouroux, Océane Asensio, Roger C. Dickey, Jérôme Fort, B. John Hughes, Vitor H. Paiva, Jaime A. Ramos, Laura Shearer, Emmanuel Tessier, Colin P. Wearn, Yves Cherel and Paco Bustamante.*

Corresponding author: fanny.cusset1@univ-lr.fr and paco.bustamante@univ-lr.fr

## Abbreviations

| | |
|---|---|
| Hg | Mercury |
| ID-GC-ICPMS | Isotope Dilution-Gaz Chromatography-Inductively Coupled Plasma Mass Spectrometry |
| GC | Gas Chromatography |
| iHg | Inorganic Hg |
| MeHg | Methyl-Hg |
| THg | Total-Hg |

# Outline

## 1) Supplementary figures

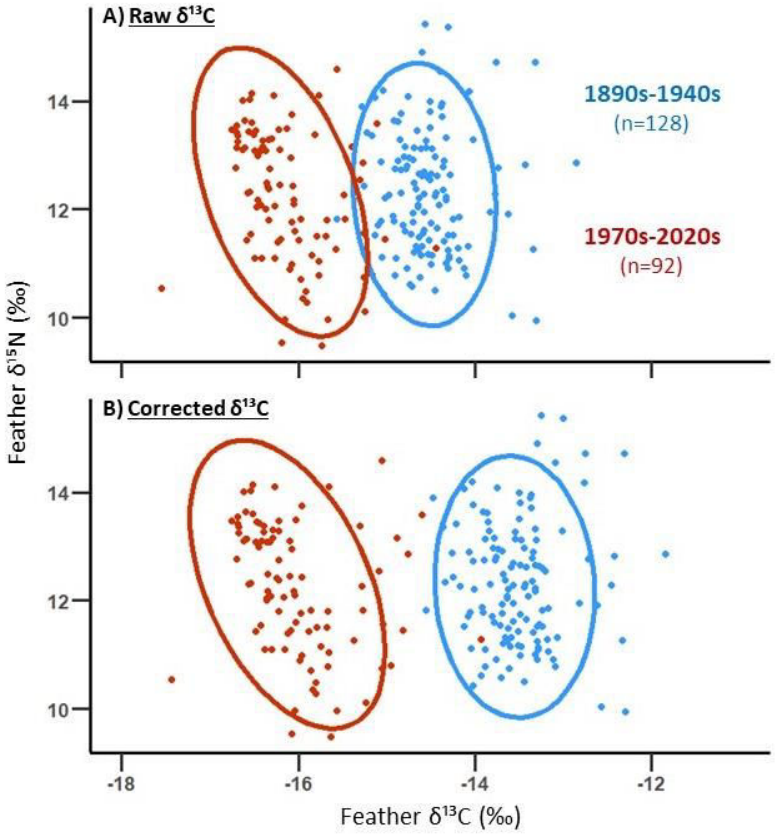


**Figure S1.** Isotopic niches of sooty terns (n=220) before (blue) and after (red) population collapse on Ascension Island (1960s-1990s), with (A) raw $\delta^{13}C$ and (B) $\delta^{13}C$ values corrected for the Suess Effect and phytoplankton fractionation (cf. details in Materials and Methods). Each ellipse includes 90% of the data.

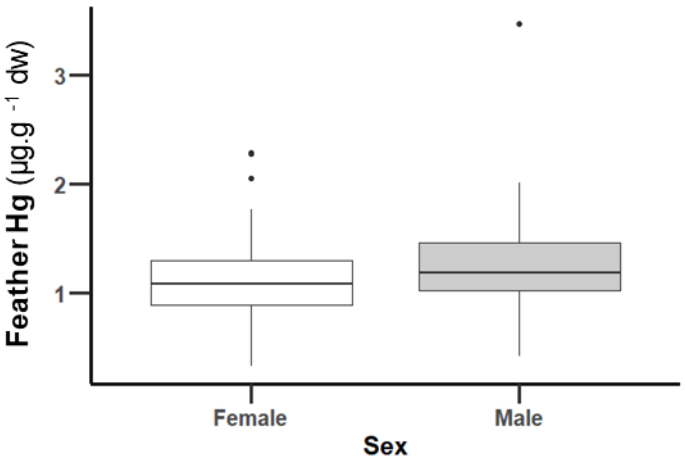


**Figure S2.** Mercury concentrations in male (grey; n=41) and female (white; n=43) sooty terns breeding on Ascension Island in 1925 (n=84). No statistical difference was detected between sexes ($F_{1,82}$=2.82, p=0.10). Boxplots indicate median values (midlines), errors bars (whiskers) and outliers (black dots).

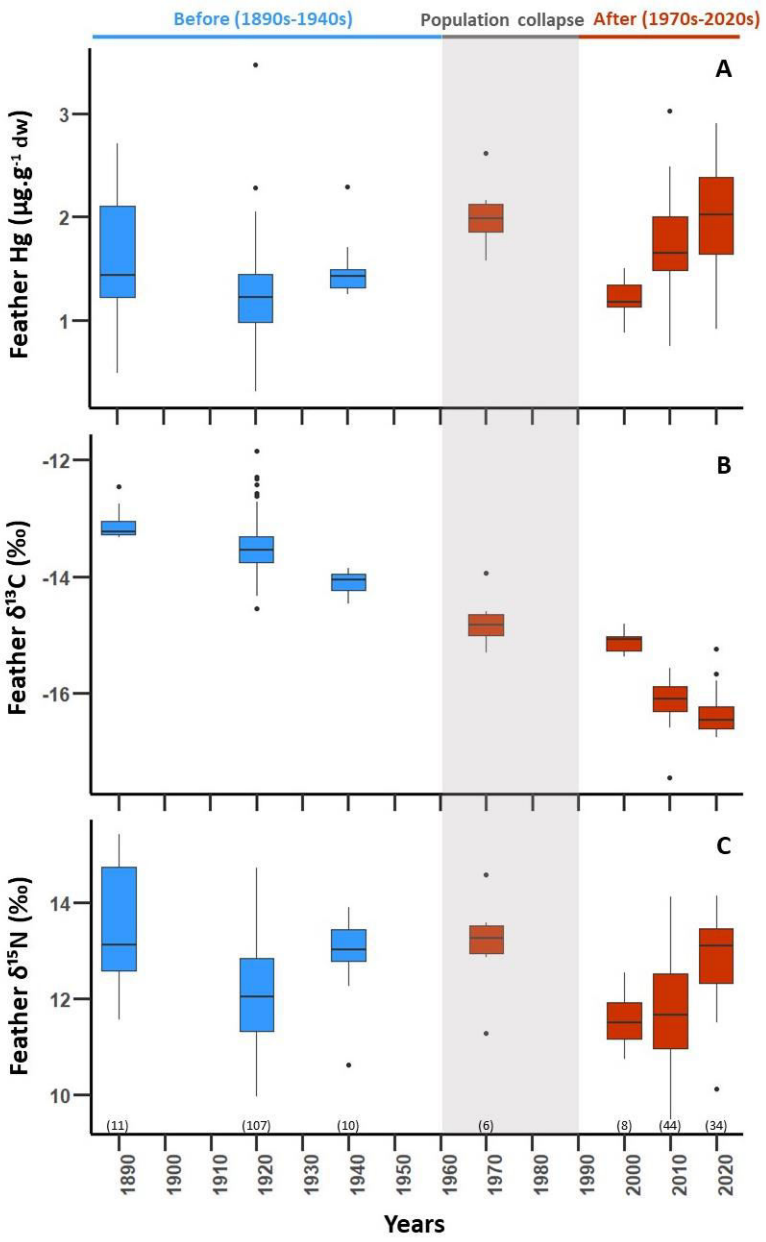


**Figure S3. (A)** Feather Hg concentrations and stable isotope values from sooty terns breeding on Ascension Island (South Atlantic Ocean) between the 1890s and the 2020s (i.e., over seven decades). **(B)** The $\delta^{13}C$ values were corrected for the Suess Effect and phytoplankton fractionation (see **Materials and Methods** section for further details) and represent a proxy for bird feeding habitat. **(C)** $\delta^{15}N$ is a proxy for bird's diet, and hence for its trophic position. Numbers in brackets represent sample sizes for each decade. The grey area represents the period where a marked population decline occurred (1960s–1990s). Birds were assigned to two main periods accordingly: before (blue) and after (red) population collapse. Boxplots indicate median values (midlines), errors bars (whiskers) and outliers (black dots).

## 2) Long-term Hg contamination in seabirds: A review

**Table S1.** Studies investigating long-term trends in Hg contamination in feathers of museum specimens. n indicates sample sizes for each species and study.

| Reference, Species | n | Feather | Time range | Site, Region (Ocean) | Main findings | Isotopes |
|---|---|---|---|---|---|---|
| **Choy et al. (2022)** | | | | | | |
| Glaucous-winged gull *(Larus glaucescens*) | 65 | Body | 1887–1996 | Salish Sea (Northeast Pacific Ocean) | No trend (stable) | Yes |
| **Bond and Lavers (2020)** | | | | | | |
| Flesh-footed shearwater *(Puffinus carneipes)* | 137 | Body | 1946–2011 | Australia (Southeast Indian Ocean) | No significant trend (-0.3 % *per* year) | No |
| **Gilmour et al. (2019)** | | | | | | |
| Gentoo penguin *(Pygoscelis papua)* | 37 | Body | 1950s–2003 | Macquarie Island, (Southern Ocean; sub-Antarctic) | No trend | No |
| King penguin *(Aptenodytes patagonicus)* | 30 | | 1940s–2003 | | Decrease | |
| Rockhopper penguin *(Eudyptes sp.)* | 34 | | 1940s–2003 | | Non-significant increase | |
| Royal penguin *(Eudyptes schlegeli)* | 42 | | 1930s–2003 | | Decrease | |
| **Gagné et al. (2019)** | | | | | | |
| Laysan albatross *(Phoebastria immutabilis)* | - | Body/ Primary | 1897–1992 | Hawaiian Islands (North Pacific Ocean), American Samoa (South Pacific Ocean), Florida Keys (Atlantic Ocean) | Decreasing from the 1980s to 2015 for Hawaiian Islands only | No |
| Bulwer's petrel *(Bulweria bulweri)* | - | | 1891–2014 | | | |
| Wedge-tailed shearwater *(Puffinus pacificus)* | - | | 1897–2014 | | | |
| White-tailed tropicbird *(Phaethon lepturus)* | - | | 1892–2015 | | | |
| Brown booby *(Sula leucogaster)* | - | | 1891–2015 | | | |
| Brown noddy *(Anous stolidus)* | - | | 1939–1996 | | | |
| White tern *(Gygis alba)* | - | | 1891–2013 | | | |
| Sooty tern *(Onychoprion fuscatus)* | - | | 1896–2015 | | | |

| | | | | | | |
|---|---|---|---|---|---|---|
| **Carravieri et al. (2016)** | | | | | | |
| Emperor penguin *(Aptenodytes forsteri)* | 28 | Body | 1950s–2007 | Adélie Land, Antarctica (Southern Ocean) | No change | Yes |
| Adelie penguin *(Pygoscelis adeliae)* | 15 | | 1950s–2007 | | Decrease (-77%) | |
| King penguin *(Aptenodytes patagonicus)* | 38 | | 1970s–2007 | Crozet Islands (Southern Ocean; sub-Antarctic waters) | No significant change (+14%) | |
| Macaroni penguin *(Eudyptes chrysolophus)* | 30 | | 1970s–2007 | | Increase (+32%) | |
| Gentoo penguin *(Pygoscelis papua)* | 24 | | 1970s–2007 | | Increase (+53%) | |
| **Bond et al. (2015)** | | | | | | |
| Ivory gull *(Pagophila eburnea)* | 80 | Body | 1877–2007 | Canadian Arctic, Greenland and Eastern Canadian waters (Arctic Ocean) | 45-fold increase (+1.6%*per* year) | Yes |
| **Vo et al. (2011)** | | | | | | |
| Black-footed albatross *(Phoebastria nigripes)* | 25 | Body | 1880–2002 | Multiples sites (North Pacific Ocean) | Increase | Yes |
| **Scheifler et al. (2005)** | | | | | | |
| King penguin *(Aptenodytes patagonicus)* | 41 | Body | 1966–2001 | Crozet Islands (Southern Ocean; sub-Antarctic waters) | Significant decrease (-34%) | No |
| **Monteiro and Furness (1997)** | | | | | | |
| Cory's shearwater *(Calonectris borealis)* | 267 | Body | 1886–1994 | Azores, Madeira, Salvages (Northeast Atlantic Ocean) | Increase by 1.1 – 1.9% *per* year | No |
| Little shearwater *(Puffinus assimilis)* | 49 | | | | - | |
| Common tern *(Sterna hirundo)* | 37 | | | | - | |
| Bulwer's petrel *(Bulweria bulweri)* | 85 | | | | Increase by 3.5 – 4.8% *per* year | |
| Madeiran storm petrel *(Oceanodroma castro)* | 63 | | | | - | |
| **Furness et al. (1995)** | | | | | | |
| Herring gull *(Larus argentatus)* | - | Body | 1880–1990 | German Bight, East Scotland, Shetland (North Sea, North Atlantic Ocean) | Increase | No |
| Common tern *(Sterna hirundo)* | - | | | | | |
| Kittiwakes *(Rissa sp.)* | - | | | | | |
| Guillemots *(Uria sp.)* | - | | | | | |
| **Thompson et al. (1993a)** | | | | | | |
| Common tern *(Sterna hirundo)* | 42 | Body | 1866–1990s | German North Sea coast, (Northeast Atlantic Ocean) | 4-fold increase in adults (+377%), 2-fold in juveniles (+139%) | No |
| Herring gull *(Larus argentatus)* | 140 | | 1884–1990s | | 2-fold increase (adults: +75%, juveniles: +110%) | |
| **Thompson et al. (1993b)** | | | | | | |
| Wandering albatross *(Diomedea exulans)* | 35 | Body | <1950–1980s | New Zealand, South Georgia, Gough Island, Marion Island (Southern Ocean; sub-Antarctic waters) | Significant increase in 3 species, but lack of widespread increase | No |
| Black-browed albatross *(Thalassarche melanorphis)* | 20 | | | | | |
| Grey-headed albatross *(Thalassarche* | 16 | | | | | |

| | | | | | | |
|---|---|---|---|---|---|---|
| *chrysotoma)* | | | | | | |
| Shy albatross *(Thalassarche cauta)* | 9 | | | | | |
| Northern giant petrel *(Macronectes halli)* | 7 | | | | | |
| Southern giant petrel *(Macronectes giganteus)* | 42 | | | | | |
| **Thompson et al. (1992)** | | | | | | |
| Northern fulmar *(Fulmarus glacialis)* | 57 | Body | 1850s–1980s | St Kilda, Foula, southern Ireland (Northeast Atlantic Ocean) | Decrease (-65% in Sheltland, -35% in St Kilda) | No |
| Manx shearwater *(Puffinus puffinus)* | 96 | | | Skomer, Wales (Northeast Atlantic Ocean) | Increase (+125%) | |
| North Atlantic gannet *(Morus bassanus)* | 57 | | | Bass Rock (North Atlantic Ocean) | Increase (+20%) | |
| Great skua *(Stercorarius skua)* | 225 | | | Foula, southern Ireland (Northeast Atlantic Ocean) | Increase (+53%) | |
| Atlantic puffin *(Fratercula arctica)* | 110 | | | St Kilda, Foula, Great Saltee, southern Ireland (Northeast Atlantic Ocean) | Increase (+120%) | |
| **Appelquist et al. (1985)** | | | | | | |
| Black guillemot *(Cepphus grille)* | 137 | Primary | 1830s–1979 | Baltic Sea, Faroe Islands, Greenland (North Atlantic Ocean) | Substantial increase | No |
| Common, Brunnich guillemots *(Uria sp.)* | 140 | | | | | |

-: Information not available in the original study

## 3) Museum sample collection

**Table S2.** Details of museums and their curators who assisted in initial enquiries about specimens of sooty tern skins collected from Ascension Island in the South Atlantic

| Name of museums | Location | Name of curators |
|---|---|---|
| **American Museum of Natural History (AMNH)** | New York, NY, USA | Tom Trombone |
| **Florida Museum of Natural History (Flor. Mus. Nat. Hist.)** | Gainesville, FL, USA | Tom Webber |
| **Peabody Museum of Natural History (Peabody)** | Yale University, New Haven, CT, USA | Kristof Zyskowski |
| **Smithonian Institution – Division of Birds (Smithonian)** | Washington DC, USA | Chris Milensky |
| **Great North Museum – Hancock Collection (Hancock)** | Newcastle upon Tyne, UK | Dan Gordon |
| **Museum of Natural Science (Mus. Nat. Sci. LSU)** | Louisiana State University, Baton Rouge, LA, USA | Steve Cardiff, Nicholas Mason |
| **National Museum of Natural History – Collection of Birds (NMNH Paris)** | Paris, France | Jérôme Fuchs |
| **National Museums Scotland (Nat. Mus. Scotland)** | Edinburgh, UK | Bob McGowan |
| **National Museum Liverpool (Nat. Mus. Liverpool)** | Liverpool, UK | Tony Parker |
| **Natural History Museum-Bird Group (NHM Tring)** | Tring, UK | Mark Adams |

2)

**Table S3.** Details of body feathers of sooty terns breeding on Ascension Island in the South Atlantic, between the 1890s and the 2020s.

Sources: **AIG** – Ascension Island Government; **AMNH** – American Museum of Natural History, New York, NY, USA; **BJH** – B. John Hughes; CPW – Colin P. Wearn; **FC** – Fanny Cusset; **Flor. Mus. Nat. Hist.** – Florida Museum of Natural History, Gainesville, FL, USA; **Hancock** – Great North Museum-Hancock Collection, Newcastle upon Tyne, UK; **Mus. Nat. Sci. LSU** – Museum of Natural Science, Louisiana State University, Baton Rouge, LA, USA; **Nat. Mus. Liverpool** – National Museums Liverpool, Liverpool, UK; **Nat. Mus. Scotland** – National Museums Scotland, Edinburgh, UK; **NHM Tring** – Natural History Museum-Bird Group, Tring, UK; **NMNH Paris** – National Museum of Natural History-Collection of Birds, Paris, France; **Peabody** – Peabody Museum of Natural History, Yale University, New Haven, CT, USA; **SJR** – S. James Reynolds; and **Smithsonian** – Smithsonian Institution-Division of Birds, Washington DC, USA.

| Sample ID | Source | Catalog number | Decade of collection |
|---|---|---|---|
| **JR1** | Hancock | B020.71 | 1890 |
| **JR2** | Nat. Mus. Scotland | NMS.Z 1956.3 (3161) | 1890 |
| **JR3** | NHM Tring | 2012.102.1 | 1890 |
| **JR4** | NHM Tring | 1880.11.18.707 | 1890 |
| **JR5** | Smithonian | USNM 118379 | 1890 |
| **JR6** | Smithonian | USNM 118380 | 1890 |
| **JR7** | Smithonian | USNM 118381 | 1890 |
| **JR8** | NHM Tring | 1894.10.28.7 | 1890 |
| **JR9** | NHM Tring | 1899.1.4.19 | 1890 |
| **JR10** | NHM Tring | 1899.1.4.20 | 1890 |
| **JR11*** | Nat. Mus. Liverpool | - | 1920 |
| **JR12** | NHM Tring | 1922.12.6.49 | 1920 |
| **JR13** | NHM Tring | 1922.12.6.50 | 1920 |
| **JR14** | Peabody | 44863 | 1920 |
| **JR15** | Peabody | 44864 | 1920 |
| **JR16** | Peabody | 44865 | 1920 |
| **JR17** | Peabody | 44866 | 1920 |
| **JR18** | Peabody | 44868 | 1920 |
| **JR19** | Peabody | 44869 | 1920 |
| **JR20** | Peabody | 44870 | 1920 |
| **JR21** | Peabody | 44871 | 1920 |
| **JR22** | Peabody | 44872 | 1920 |
| **JR23** | Peabody | 44873 | 1920 |
| **JR24** | Peabody | 44874 | 1920 |
| **JR25** | Peabody | 44875 | 1920 |
| **JR26** | Peabody | 44876 | 1920 |

| | | | |
|---|---|---|---|
| **JR27** | Peabody | 44877 | 1920 |
| **JR28** | Peabody | 44878 | 1920 |
| **JR29** | Peabody | 44879 | 1920 |
| **JR30** | Peabody | 44888 | 1920 |
| **JR31** | Peabody | 44889 | 1920 |
| **JR32** | Peabody | 44890 | 1920 |
| **JR33** | Peabody | 44891 | 1920 |
| **JR34** | Peabody | 44892 | 1920 |
| **JR35** | Peabody | 44893 | 1920 |
| **JR36** | Peabody | 44894 | 1920 |
| **JR37** | Peabody | 44895 | 1920 |
| **JR38** | Peabody | 44896 | 1920 |
| **JR39** | Peabody | 44897 | 1920 |
| **JR40** | Peabody | 44898 | 1920 |
| **JR41** | Peabody | 44899 | 1920 |
| **JR42** | Peabody | 44901 | 1920 |
| **JR43** | Peabody | 44902 | 1920 |
| **JR44** | Peabody | 44903 | 1920 |
| **JR45** | Peabody | 44904 | 1920 |
| **JR46** | Peabody | 44905 | 1920 |
| **JR47** | Peabody | 44906 | 1920 |
| **JR48** | Peabody | 44907 | 1920 |
| **JR49** | Peabody | 44908 | 1920 |
| **JR50** | Peabody | 44909 | 1920 |
| **JR51** | Peabody | 44921 | 1920 |
| **JR52** | Peabody | 44922 | 1920 |
| **JR53** | Peabody | 44923 | 1920 |
| **JR54** | Peabody | 44924 | 1920 |
| **JR55** | Peabody | 44925 | 1920 |
| **JR56** | Peabody | 44934 | 1920 |
| **JR57** | Peabody | 44935 | 1920 |
| **JR58** | Peabody | 44936 | 1920 |
| **JR59** | Peabody | 44937 | 1920 |
| **JR60** | Peabody | 44938 | 1920 |
| **JR61** | Peabody | 44939 | 1920 |
| **JR62** | Peabody | 44940 | 1920 |
| **JR63** | Peabody | 44941 | 1920 |
| **JR64** | Peabody | 44942 | 1920 |
| **JR65** | Peabody | 44943 | 1920 |
| **JR66** | Peabody | 44944 | 1920 |
| **JR67** | Peabody | 44945 | 1920 |
| **JR68** | Peabody | 44946 | 1920 |
| **JR69** | Peabody | 44947 | 1920 |
| **JR70** | Peabody | 44948 | 1920 |

| | | | |
|---|---|---|---|
| **JR71** | Peabody | 44949 | 1920 |
| **JR72** | Peabody | 44950 | 1920 |
| **JR73** | Peabody | 44951 | 1920 |
| **JR74** | Peabody | 44952 | 1920 |
| **JR75** | Peabody | 44953 | 1920 |
| **JR76** | Peabody | 44954 | 1920 |
| **JR77** | Peabody | 44955 | 1920 |
| **JR78** | Peabody | 44956 | 1920 |
| **JR79** | Peabody | 44967 | 1920 |
| **JR80** | Peabody | 44968 | 1920 |
| **JR81** | Peabody | 44969 | 1920 |
| **JR82** | Peabody | 44970 | 1920 |
| **JR83** | Peabody | 44971 | 1920 |
| **JR84** | Peabody | 44972 | 1920 |
| **JR85** | Peabody | 44973 | 1920 |
| **JR86** | Peabody | 44974 | 1920 |
| **JR87** | Peabody | 44975 | 1920 |
| **JR88** | Peabody | 44976 | 1920 |
| **JR89** | Peabody | 44977 | 1920 |
| **JR90** | Peabody | 44978 | 1920 |
| **JR91** | Peabody | 44981 | 1920 |
| **JR92** | Peabody | 44982 | 1920 |
| **JR93** | Peabody | 44983 | 1920 |
| **JR94** | Peabody | 44984 | 1920 |
| **JR95** | Peabody | 44985 | 1920 |
| **JR96** | AMNH | 269206 | 1920 |
| **JR97** | AMNH | 269227 | 1920 |
| **JR98** | AMNH | 269226 | 1920 |
| **JR99** | AMNH | 269225 | 1920 |
| **JR100** | AMNH | 269224 | 1920 |
| **JR101** | AMNH | 269223 | 1920 |
| **JR102** | AMNH | 269222 | 1920 |
| **JR103** | AMNH | 269221 | 1920 |
| **JR104** | AMNH | 269220 | 1920 |
| **JR105** | AMNH | 269219 | 1920 |
| **JR106** | AMNH | 269218 | 1920 |
| **JR107** | AMNH | 269217 | 1920 |
| **JR108** | AMNH | 269216 | 1920 |
| **JR109** | AMNH | 269215 | 1920 |
| **JR110** | AMNH | 269214 | 1920 |
| **JR111** | AMNH | 269213 | 1920 |
| **JR112** | AMNH | 269212 | 1920 |
| **JR113** | AMNH | 269211 | 1920 |
| **JR114** | AMNH | 269210 | 1920 |

| | | | |
|---|---|---|---|
| **JR115** | AMNH | 269209 | 1920 |
| **JR116** | AMNH | 269208 | 1920 |
| **JR117** | AMNH | 269207 | 1920 |
| **JR118** | AMNH | 308427 | 1940 |
| **JR119** | AMNH | 308426 | 1940 |
| **JR120** | AMNH | 308425 | 1940 |
| **JR121** | AMNH | 308424 | 1940 |
| **JR122** | AMNH | 308423 | 1940 |
| **JR123** | AMNH | 308422 | 1940 |
| **JR124** | AMNH | 308421 | 1940 |
| **JR125** | AMNH | 308428 | 1940 |
| **JR126** | AMNH | 308429 | 1940 |
| **JR127** | Nat. Sci. LSU | 73125 | 1940 |
| **JR128** | NHM Tring | 1962.42.2 | 1970 |
| **JR129** | Smithsonian | 534287 | 1970 |
| **JR130** | Smithsonian | 534285 | 1970 |
| **JR131** | Smithsonian | 534286 | 1970 |
| **JR132** | Smithsonian | 534288 | 1970 |
| **JR133** | BJH | - | 2000 |
| **JR134** | BJH | - | 2000 |
| **JR135** | BJH | - | 2000 |
| **JR136** | BJH | - | 2000 |
| **JR137** | BJH | - | 2000 |
| **JR138** | BJH | - | 2000 |
| **JR139** | BJH | - | 2000 |
| **JR140** | BJH | - | 2000 |
| **JR141** | NMNH Paris | CG 1973-286 | 1890 |
| **JR142** | Flor. Mus. Nat. His. | UF 37533 | 1970 |
| **JR143** | CPW/SJR | - | 2010 |
| **JR144** | CPW/SJR | - | 2010 |
| **JR145** | CPW/SJR | - | 2010 |
| **JR146** | CPW/SJR | - | 2010 |
| **JR147** | CPW/SJR | - | 2010 |
| **JR148** | CPW/SJR | - | 2010 |
| **JR149** | CPW/SJR | - | 2010 |
| **JR150** | CPW/SJR | - | 2010 |
| **JR151** | CPW/SJR | - | 2010 |
| **JR152** | CPW/SJR | - | 2010 |
| **JR153** | CPW/SJR | - | 2010 |
| **JR154** | CPW/SJR | - | 2010 |
| **JR155** | CPW/SJR | - | 2010 |
| **JR156** | CPW/SJR | - | 2010 |
| **JR157** | CPW/SJR | - | 2010 |
| **JR158** | CPW/SJR | - | 2010 |

| | | | |
|---|---|---|---|
| **JR159** | CPW/SJR | - | 2010 |
| **JR160** | CPW/SJR | - | 2010 |
| **JR161** | CPW/SJR | - | 2010 |
| **JR162** | CPW/SJR | - | 2010 |
| **JR163** | CPW/SJR | - | 2010 |
| **JR164** | CPW/SJR | - | 2010 |
| **JR165** | CPW/SJR | - | 2010 |
| **JR166** | CPW/SJR | - | 2010 |
| **JR167** | CPW/SJR | - | 2010 |
| **JR168** | CPW/SJR | - | 2010 |
| **JR169** | CPW/SJR | - | 2010 |
| **JR170** | CPW/SJR | - | 2010 |
| **JR171** | CPW/SJR | - | 2010 |
| **JR172** | CPW/SJR | - | 2010 |
| **JR173** | CPW/SJR | - | 2010 |
| **JR174** | CPW/SJR | - | 2010 |
| **JR175** | CPW/SJR | - | 2010 |
| **JR176** | CPW/SJR | - | 2010 |
| **JR177** | CPW/SJR | - | 2010 |
| **JR178** | CPW/SJR | - | 2010 |
| **JR179** | CPW/SJR | - | 2010 |
| **JR180** | CPW/SJR | - | 2010 |
| **JR181** | CPW/SJR | - | 2010 |
| **JR182** | CPW/SJR | - | 2010 |
| **JR183** | CPW/SJR | - | 2010 |
| **JR185** | CPW/SJR | - | 2010 |
| **JR186** | CPW/SJR | - | 2010 |
| **JR187** | CPW/SJR | - | 2010 |
| **FCa31** | FC/AIG | - | 2020 |
| **FCa32** | FC/AIG | - | 2020 |
| **FCa33** | FC/AIG | - | 2020 |
| **FCa34** | FC/AIG | - | 2020 |
| **FCa35** | FC/AIG | - | 2020 |
| **FCb16** | FC/AIG | - | 2020 |
| **FCb17** | FC/AIG | - | 2020 |
| **FCb18** | FC/AIG | - | 2020 |
| **FCb19** | FC/AIG | - | 2020 |
| **FCb20** | FC/AIG | - | 2020 |
| **FCb21** | FC/AIG | - | 2020 |
| **FCb22** | FC/AIG | - | 2020 |
| **FCb23** | FC/AIG | - | 2020 |
| **FCb24** | FC/AIG | - | 2020 |
| **FCb25** | FC/AIG | - | 2020 |
| **FCb26** | FC/AIG | - | 2020 |

| | | | |
|---|---|---|---|
| **FCb27** | FC/AIG | - | 2020 |
| **FCb28** | FC/AIG | - | 2020 |
| **FCb29** | FC/AIG | - | 2020 |
| **FCb30** | FC/AIG | - | 2020 |
| **FCb31** | FC/AIG | - | 2020 |
| **FCb32** | FC/AIG | - | 2020 |
| **FCb33** | FC/AIG | - | 2020 |
| **FCb34** | FC/AIG | - | 2020 |
| **FCb36** | FC/AIG | - | 2020 |
| **FCb37** | FC/AIG | - | 2020 |
| **FCb38** | FC/AIG | - | 2020 |
| **FCb39** | FC/AIG | - | 2020 |
| **FCb40** | FC/AIG | - | 2020 |
| **FCb41** | FC/AIG | - | 2020 |
| **FCb42** | FC/AIG | - | 2020 |
| **FCb43** | FC/AIG | - | 2020 |
| **FCb44** | FC/AIG | - | 2020 |
| **FCb45** | FC/AIG | - | 2020 |

***** Sample omitted from statistical analyses as it was identified as an outlier.

## 4) <u>Museum inorganic contamination in old specimens</u>

**Context**. Total-Hg (THg) includes two main forms: inorganic Hg (iHg) and methyl-Hg (MeHg). In bird feathers, the dominant form of THg is MeHg (>90%). For this reason, THg is routinely measured in bird feathers, as a proxy for bird MeHg burden.

Historically, iHg salts were used as preservatives in museum collections until approximately the 1970s and as a result represent a major bias in Hg quantification in older bird specimens. Measuring THg in old specimens is thus inappropriate. Therefore, analysing MeHg specifically is the best alternative to investigate Hg temporal trends in museum-archived bird specimens.

**Methods- Hg speciation analyses.** Mercury speciation analyses were performed following established methodology presented in Renedo et al. (2017). In this study, Hg species (iHg and MeHg) were extracted from feather homogenates by acid microwave digestion in 3 mL of suprapure grade nitric acid solution ($HNO_3$ 6N), characterized by 1 min of heating to 75°C and 4 min at 75°C (Discover SP-D, CEM Corporation, USA) in CEM Pyrex vessels, with magnetic agitation to homogenise samples and after a predigestion step overnight at room temperature. Sample mass fractions and $HNO_3$ 6N volumes were precisely weighted using a $10^{-5}$ analytical balance. Then, sample extracts underwent a derivatization step at pH 3.9 in order to allow liquid/liquid extraction of the Hg species in GC solvent and its subsequent chromatographic elution. Ethylation was thus achieved by adding to the sample extracts 5 mL of buffer solution (Acetic/Acetate, 0.1 M, pH 3.9) and small amounts of ultrapure grade $NH_3$ or HCl to reach pH=3.9 (3.85-4.05). GC solvent (isooctane, 300 µL) and $NaBEt_4$ (80 µL, 5%) were finally added before agitation (20 min, elliptic table) and centrifugation (2500 rpm, 3 min). The resulting organic phase was retrieved and transferred to GC vials. Final extracts were stored in the freezer (-20°C) prior GC analyses.

In order to achieve accurate and precise Hg speciation analyses on bird feather specimens, the Isotopic Dilution methodology was applied to correct efficiently the matrix effects and Hg artefacts during the sample preparation. Before the microwave extraction, samples were thus spiked with known amounts of two enriched isotope tracer solutions (ISC-Science, Spain), namely $^{199}$iHg and $^{201}$MeHg, to alter the natural isotopic abundance of the studied endogenous species ($^{202}$iHg and $^{202}$MeHg). Mixed isotope ratios were then quantified, as explained elsewhere (Clémens et al., 2012; Rodríguez-González et al., 2005). Mercury species analyses were carried out by GC-ICPMS Trace Ultra GC, equipped with a Triplus RSH autosampler coupled to an ICP-

MS XSeries II (ThermoFisher Scientific, USA). The reported results of [THg] were calculated as the sum of [MeHg] and [iHg] determined by ID-GC-ICPMS and were compared to [THg] determined by AMA-254, to evaluate their similarity and verify the recovery of the extraction. Human hair certified reference material (NIES-13) was analysed during each analytical session to assess the robustness of the methodology. The certified values of NIES-13 were: [THg] = 4.42 ± 0.20 μg $g^{-1}$ and [MeHg] = 3.80 ± 0.40 μg $g^{-1}$).

**Table S4.** Tests for Hg speciation analyses of feathers from free-living birds (n=3) and museum specimens (n=3) specimens of sooty terns breeding on Ascension Island. Values are means ± SD. Concentrations are expressed in μg $g^{-1}$ dw for methyl-Hg (MeHg), inorganic Hg (iHg), total-Hg obtained from Hg speciation analyses (Σ MeHg+iHg) and from AMA analyses (THg). Recovery is calculated as (Σ MeHg + iHg)×100 / THg. Samples were analysed in duplicate/triplicates, with certified reference material (NIES-13). Further details are provided in the **Materials and Methods**.

| Year | ID | MeHg | iHg | Σ MeHg+iHg | THg | Recovery (%) |
|---|---|---|---|---|---|---|
| 2000 | 1A | 1.24 ± 0.04 | 0.020 ± 0.001 | 1.26 ± 0.09 | 1.24 | 102 |
| 2000 | 1C | 0.84 ± 0.03 | 0.002 ± 0.001 | 0.86 ± 0.09 | 0.93 | 92 |
| 2000 | 1F | 1.31 ± 0.03 | 0.031 ± 0.002 | 1.34 ± 0.10 | 1.42 | 94 |
| 1877 | JR3 | 0.49 ± 0.02 | 24.62 ± 0.34 | 25.11 ± 1.33 | 27.84 | 92 |
| 1890 | JR5 | 0.69 ± 0.09 | 16.06 ± 0.07 | 16.75 ± 2.16 | 17.63 | 95 |
| 1925 | JR74 | 0.57 ± 0.01 | 2.66 ± 0.05 | 3.24 ± 0.12 | 3.39 | 96 |
| **NIES-13** | certified | 3.80 ± 0.40 | 0.62 ± 0.60 | 4.42 ± 0.20 | 4.42 | 100 |
| | measured | 3.64 ± 0.02 | 0.89 ± 0.02 | 4.53 ± 0.11 | 4.42 | 103 |

**Results**. To test method validation on museum specimens, Hg speciation analyses were performed on three museum specimens (dating from 1877, 1890, 1925) and three free-living birds (from 2000) (Table S3). Average recoveries (Σ MeHg + iHg determined by GC-ICPMS

*versus* THg determined by AMA) were 96.13 ± 4.88% (range: 92–102%) for feathers from the 2000s and 94.11 ± 1.99% (range: 92–96%) for feathers from museum specimens, proving method robustness. Mercury species distribution in old specimens was 92.1 ± 8.5% (range: 82.3–98.1%) iHg and 7.9 ± 8.5% (1.9–17.7%) MeHg. In recent specimens, iHg represented only 2.0 ± 0.4% (range: 1.6–2.3%) of the THg burden and MeHg 98.0 ± 0.4% (range: 97.7–98.4%), thus confirming the use of inorganic Hg salts as museum preservatives.

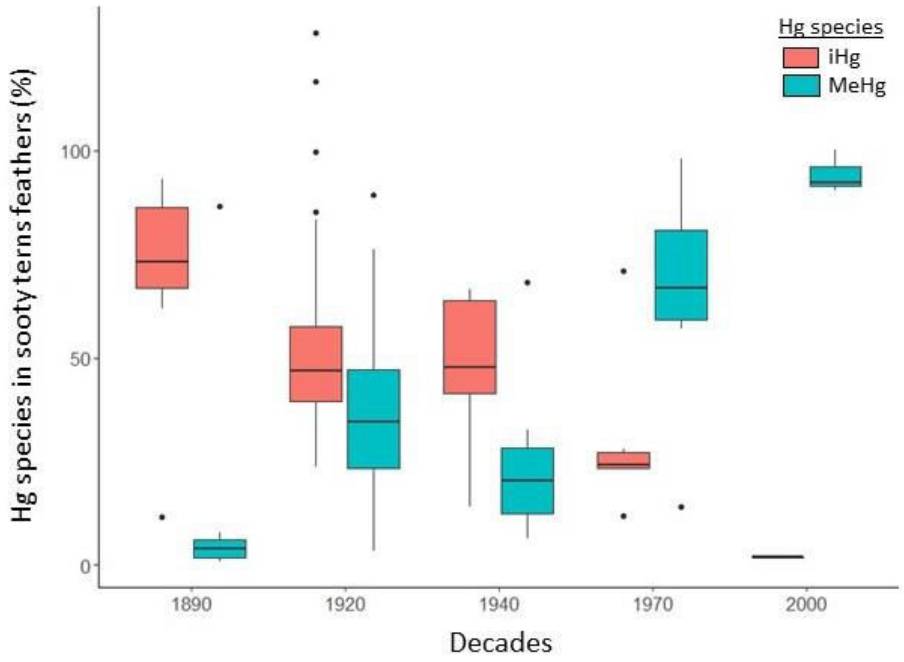


**Figure S4.** Percentage of different Hg species (inorganic Hg, iHg in red; methyl-Hg, MeHg in blue) in feathers of museum skins and free-living sooty terns breeding on Ascension Island, over 145 years. The sum of Hg (equivalent to total-Hg, THg) species is 100%.

Overall, THg (AMA-254) concentrations ranged from 0.75 to 264.92 µg $g^{-1}$ dw (Table 1), with highest values in old specimens (1890s: 70.12 ± 87.34 µg $g^{-1}$ dw, n=11). Figure S1 provides

details of %iHg and %MeHg for all samples over time, highlighting that museum preservation processes used inorganic Hg salt for skin conservation. Table S4 provides details on Hg speciation analyses, with mean ± SD (range) values for all Hg species and recoveries.

**Table S5.** Summary of Hg speciation analyses of sooty tern feathers from Ascension Island (1876−2021): methyl-Hg (MeHg), inorganic Hg (iHg) and the sum of both (equivalent to total-Hg, THg). Values are means ± SD (range). Concentrations (µg $g^{-1}$ dw) were quantified in all samples and in certified reference material (NIES-13). n indicates sample sizes. Individual recovery (%) is calculated as: (Σ MeHg + iHg)×100 / THg. Further details are provided in the **Materials and Methods**.

| | **MeHg** | **iHg** | **Σ MeHg + iHg** | **THg** | **Recovery (%)** |
|---|---|---|---|---|---|
| **Samples** (n=131) | 1.3 ± 0.5 (0.3-3.5) | 7.4 ± 26.5 (0.2-246.4) | 8.8 ± 26.8 (1.2-249.1) | 10.8 ± 31.1 (1.7-264.9) | -* |
| **NIES-13** (n=3) | 3.6 ± 0.1 (3.6-3.7) | 0.7 ± 0.2 (0.5-0.9) | 4.3 ± 0.3 (4.0-4.5) | 4.42 ± 0.01 | 97.7 ± 5.8 (91.3-102.5) |

*No recovery is provided for the samples, because of the high inorganic contamination in old specimens which completely biased the recovery percentage.

## 5) <u>Empirical calculations of percentages of change</u>

To enable trend comparison with published literature, we calculated the percentage of evolution (increase or decrease) between decades, for each evolution phase identified by GAM temporal trends and globally (i.e., between the 1920s and the 2020s). Negative and positive percentages correspond to a decrease and an increase, respectively. For example, between the 1920s and the 1970s, E.S1 applies as follows:

$$\%\text{change (increase)} = ([Hg]_{1970s} - [Hg]_{1920s}) / [Hg]_{1970s} \quad \text{(E.S1)}$$

The overall percentage (for the entire period) was then converted into a % *per* year by dividing by the number of years (n=100).

**Table S6.** Percentage of change in temporal trends of Hg, $\delta^{13}C$ and $\delta^{15}N$ values between different focal periods of the study. Positive and negative values indicate increasing and decreasing metrics during each focal period, respectively. Following GAMs analyses, only periods in bold are scientifically appropriate (realistic) for interpretation.

| **Focal periods** | **Hg (%)** | **$\delta^{13}C$ (%)** | **$\delta^{15}N$ (%)** |
|---|---|---|---|
| 1890s – 1920s | - 23.9 | - 3.0 | - 10.4 |
| **1920s – 1970s** | **+ 62.9** | **- 4.4** | - |
| 1970s – 2000s | - | - 4.7 | - |
| **2000 – 2020s** | **+ 62.8** | **- 2.4** | **+ 11.5** |
| Before *versus* after population collapse | + 38.8 | - 18.6 | - 0.7 |
| 1920s *versus* 2020s | + 37.1 | - 17.4 | + 5.7 |

Example: Mean Hg concentrations decreased by 23.9% between the 1890s and the 1920s.

## 6) Statistics - Generalized Additive Models (GAMs)

**Table S7.** Outputs from GAM models explaining variation in feather Hg and stable isotope values between the 1890s and the 2020s in adult sooty terns breeding on Ascension Island in the South Atlantic Ocean. For the intercept, values are estimates and standard errors. For the smoother (year), values are effective degrees of freedom. K indicates the number of knots in temporal trends of each variable.

| Response variable | Intercept | k | s(Year) | p-value | Deviance explained (%) |
|---|---|---|---|---|---|
| Hg | 1.59 ± 0.04 | 5 | 3.61 | <0.0001*** | 25.1 |
| $\delta^{13}C$ | -14.91 ± 0.03 | 5 | 3.39 | <0.0001*** | 12.5 |
| $\delta^{15}N$ | 12.38 ± 0.09 | 5 | 3.67 | <0.0001*** | 91.0 |

## 7) References


Appelquist, H., Drabæk, I., Asbirk, S., 1985. Variation in mercury content of Guillemot feathers over 150 years. Mar. Pollut. Bull. 16, 244–248.

Bond, A.L., Hobson, K.A., Branfireun, B.A., 2015. Rapidly increasing methyl mercury in endangered ivory gull (Pagophila eburnea) feathers over a 130 year record. Proc. Biol. Sci. 282, 1–8.

Bond, A.L., Lavers, J.L., 2020. Biological archives reveal contrasting patterns in trace element concentrations in pelagic seabird feathers over more than a century. Environ. Pollut. 263, 114631.

Carravieri, A., Cherel, Y., Jaeger, A., Churlaud, C., Bustamante, P., 2016. Penguins as bioindicators of mercury contamination in the southern Indian Ocean: geographical and temporal trends. Environ. Pollut. Barking Essex 1987 213, 195–205.

Clémens, S., Monperrus, M., Donard, O.F.X., Amouroux, D., Guérin, T., 2012. Mercury speciation in seafood using isotope dilution analysis: A review. Talanta 89, 12–20.

Furness, R.W., Thompson, D.R., Becker, P.H., 1995. Spatial and temporal variation in mercury contamination of seabirds in the North Sea. Helgoländer Meeresunters. 49, 605–615.

Gagné, T.O., Johnson, E.M., Hyrenbach, K.D., Hagemann, M.E., Bass, O.L., MacDonald, M., Peck, B., Houtan, K.S.V., 2019. Coupled trophic and contaminant analysis in seabirds through space and time. Environ. Res. Commun. 1, 111006.

Gilmour, M.E., Holmes, N.D., Fleishman, A.B., Kriwoken, L.K., 2019. Temporal and interspecific variation in feather mercury in four penguin species from Macquarie Island, Australia. Mar. Pollut. Bull. 142, 282–289.

Monteiro, L.R., Furness, R.W., 1997. Accelerated increase in mercury contamination in north Atlantic mesopelagic food chains as indicated by time series of seabird feathers. Environ. Toxicol. Chem. 16, 2489–2493.

Renedo, M., Bustamante, P., Tessier, E., Pedrero, Z., Cherel, Y., Amouroux, D., 2017. Assessment of mercury speciation in feathers using species-specific isotope dilution analysis. Talanta 174, 100–110.

Rodríguez-González, P., Marchante-Gayón, J.M., García Alonso, J.I., Sanz-Medel, A., 2005. Isotope dilution analysis for elemental speciation: A tutorial review. Spectrochim. Acta Part B At. Spectrosc. 60, 151–207.

Scheifler, R., Gauthier-Clerc, M., Bohec, C.L., Crini, N., Cœurdassier, M., Badot, P.-M., Giraudoux, P., Maho, Y.L., 2005. Mercury concentrations in king penguin (Aptenodytes patagonicus) feathers at Crozet Islands (sub-Antarctic): Temporal trend between 1966–1974 and 2000–2001. Environ. Toxicol. Chem. 24, 125–128.

Thompson, D.R., Becker, P.H., Furness, R.W., 1993a. Long-Term changes in mercury concentrations in herring gulls *Larus argentatus* and common terns *Sterna hirundo* from the German North Sea Coast. J. Appl. Ecol. 30, 316–320.

Thompson, D.R., Furness, R.W., Lewis, S.A., 1993b. Temporal and spatial variation in mercury concentrations in some albatrosses and petrels from the sub-Antarctic. Polar Biol. 13, 239–244.

Thompson, D.R., Furness, R.W., Walsh, P.M., 1992. Historical changes in mercury concentrations in the marine ecosystem of the North and North-East Atlantic Ocean as indicated by seabird feathers. J. Appl. Ecol. 29, 79–84.

Vo, A.-T.E., Bank, M.S., Shine, J.P., Edwards, S.V., 2011. Temporal increase in organic mercury in an endangered pelagic seabird assessed by century-old museum specimens. Proc. Natl. Acad. Sci. USA. 108, 7466–7471.